ANALYSIS OF DUAL BAND RECTANGULAR MICROSTRIPANTENNA USING IE3D/PSO

A THESIS

SUBMITTED IN PARTIAL FULFILLMENT OF THE

REQUIREMENTS FOR THE DEGREE OF

MASTER OF TECHNOLOGY

IN

TELEMATICS AND SIGNAL PROCESSING

BY

YOGESH KUMAR CHOUKIKER

Regd. No. - 207EC104

Department of Electronics and Communication Engineering

National Institute of Technology

Rourkela-769008

2009

ANALYSIS OF DUAL BAND RECTANGULAR MICROSTRIPANTENNA USING IE3D/PSO

A THESIS

SUBMITTED IN PARTIAL FULFILLMENT OF THE

REQUIREMENTS FOR THE DEGREE OF

MASTER OF TECHNOLOGY

IN

TELEMATICS AND SIGNAL PROCESSING

BY

YOGESH KUMAR CHOUKIKER

207EC104

UNDER THE GUIDANCE OF

PROF. S K BEHERA

Department of Electronics and Communication Engineering

National Institute of Technology

Rourkela-769008

2009

Dedicated to my Grandfather

Department of Electronics & Communication Engineering
National Institute of Technology Rourkela

Date: 28.05.2009

CERTIFICATE

This is to certify that the thesis entitled**, "Analysis of Dual Band Rectangular Microstrip Antenna Using IE3D\PSO"** submitted by Mr. **Yogesh Kumar Choukiker** in partial fulfillment of the requirements for the award of Master of Technology Degree in Electronics and Communication Engineering with specialization in **"Telematics and Signal Processing"** during session 2008-09 at the National Institute of Technology, Rourkela (Deemed University) is an authentic work carried out by him under my supervision and guidance.

To the best of my knowledge, the matter embodied in the thesis has not been submitted to any other University/ Institute for the award of any degree or diploma.

Prof. S K Behera

ACKNOWLEDGEMENTS

This project is by far the most significant accomplishment in my life and it would be impossible without people who supported me and believed in me.

I would like to extend my gratitude and my sincere thanks to my honorable, esteemed supervisor **Prof. S K Behera**. He is not only a great teacher/professor with deep vision but also and most importantly a kind person. I sincerely thank for his exemplary guidance and encouragement. His trust and support inspired me in the most important moments of making right decisions and I am glad to work with him. My special thank goes to **Prof. S K Patra** Head of the Department of Electronics and Communication Engineering, NIT, Rourkela, for providing us with best facilities in the Department and his timely suggestions.

I want to thank all my teachers **Prof. G.S. Rath**, **Prof G Panda**, **Prof. K. K. Mahapatra, Prof. S.K. Meher and Prof. P K Sahu** for providing a solid background for my studies and research thereafter. They have been great sources of inspiration to me and I thank them from the bottom of my heart.

I would like to thank all my friends and especially my classmates for all the thoughtful and mind stimulating discussions we had, which prompted us to think beyond the obvious. I have enjoyed their companionship so much during my stay at NIT, Rourkela.

I would like to thank all those who made my stay in Rourkela an unforgettable and rewarding experience.

Last but not least I would like to thank my parents, who taught me the value of hard work by their own example. They rendered me enormous support during the whole tenure of my stay in NIT Rourkela.

Yogesh Kumar Choukiker

CONTENTS

ABSTRACT

The thesis covers three aspects of Microstrip antenna designs. The first is the analysis and design of single element rectangular Microstrip antenna which operates at the central frequency of 2.4 GHz and the second aspect is the design of dual band rectangular Microstrip antenna which is operates as 2.4 & 3.08 GHz. Both antennas have been modeled, designed and simulated. Basically, transmission line and cavity modeling is going to use to model both antennas. First, the design parameters for single element of rectangular patch antenna have been calculated from the transmission line model equation and extend the antenna design to Dual Band rectangular Microstrip patch antenna using the slots at radiating edge. The simulation process has been done through IE3D electromagnetic software which is based on method of movement (MOM).For rectangular Microstrip antenna design used RT- Duriod which is Teflon based, Microstrip board with dielectric constant 2.4 and the substrate height is 1.58 mm, scaling factor 0.95 and loss tangent is 0.001. The properties of antenna such as bandwidth, S-Parameter has been investigated and compared between different optimization scheme and theoretical results.

The third is the interfacing between IE3D\PSO (MATLAB).In this part optimization is done through Partical Swarm Optimization (PSO) algorithm using IE3D simulation software. Particle-swarm optimization was developed in 1995 and models the movement and intelligence of swarms. Behind the algorithm are a social psychologist and an electrical engineer, who developed the optimizer inspired by nature. The technique has proven successful for many electromagnetic problems and is a robust and stochastic search method.

The particle-swarm algorithm worked well on several problems. It was used for optimizing mathematical functions and electromagnetic problems. The optimized antennas were determined to have desired resonant frequencies, high gain, and low weight and return losses. The patch antennas turned out to be troublesome to handle, thus some improvements such as inclusion of ground planes, are discussed.

List of Figures and Tables

Figures

Tables

CHAPTER 1

THESIS OVERVIEW

1.1 Introduction

Satellite communication and Wireless communication has been developed rapidly in the past decades and it has already a dramatic impact on human life. In the last few years, the development of wireless local area networks (WLAN) represented one of the principal interests in the information and communication field. Thus, the current trend in commercial and government communication systems has been to develop low cost, minimal weight, low profile antennas that are capable of maintaining high performance over a large spectrum of frequencies. This technological trend has focused much effort into the design of Microstrip (patch) antennas [1]. With a simple geometry, patch antennas offer many advantages not commonly exhibited in other antenna configurations. For example, they are extremely low profile, lightweight, simple and inexpensive to fabricate using modern day printed circuit board technology, compatible with microwave and millimeter-wave integrated circuits (MMIC), and have the ability to conform to planar and non planar surfaces. In addition, once the shape and operating mode of the patch are selected, designs become very versatile in terms of operating frequency, polarization, pattern, and impedance. The variety in design that is possible with Microstrip antenna probably exceeds that of any other type of antenna element.

Using the Dual Band Microstrip Antenna concept in this thesis dual band rectangular Microstrip antenna is designed simulated and tested. There are a few software available which allow the optimization of the antenna. IE3D one of the most imperial electromagnetic software which allows to solving for radio and microwave application. It works based on method of movement (MOM) .The simulator tool computes most of the useful quantities of interest such as radiation pattern, input impedance and gain etc.

This thesis attempts to confirm the low frequency ratio of Dual Band Microstrip Antenna by designing the single element rectangular Microstrip antenna. Also one of most important work is done in this thesis is the optimization of rectangular Microstrip antenna Single Band and Dual Band both using interfacing between **IE3D\PSO**.

1.2 Thesis motivation

With bandwidths as low as a few percent, broadband applications using conventional Microstrip patch designs are limited. Other drawbacks of patch antennas include low efficiency, limited power capacity, spurious feed radiation, poor polarization purity, narrow bandwidth, and manufacturing tolerance problems. For over two decades, research scientists have developed several methods to increase the bandwidth and low frequency ratio of a patch antenna. Many of these techniques involve adjusting the placement and/or type of element used to feed (or excite) the antenna.

Dual-frequency operation of antennas has become a necessity for many applications in recent wireless communication systems, such as GPS, GSM services operating at two different frequency bands. In satellite communication, antennas with low frequency ratio are very much essential. A dual-frequency patch antenna with an inset feed can produce a dual-frequency response, with both frequencies having the same polarization sense with a low frequency ratio. It is also less sensitive to feed position, which allows the use of an inset planar feed.

While optimizing the antenna parameters, using IE3D, the overlapping problem is most often encountered.. There are several other techniques to optimize the antenna parameters such as:

(i) Genetic Algorithm (ii) Particle Swarm Optimization (PSO) (iii) Simulated Annealing etc. The PSO algorithm and its variations have been found to be very suitable and relatively better method for optimization of electromagnetic problems. Thus, it is expected that a best possible

optimization may be obtained by further refinement of the IE3D results with the help of PSO. Using the combination of IE3D and PSO algorithm, a design technique for patch antenna has been developed.

1.3 Literature Review and Methodology

The invention of Microstrip patch antennas has been attributed to several authors, but it was certainly dates in the 1960s with the first works published by Deschamps, Greig and Engleman, and Lewin, among others. After the 1970's research publications started to flow with the appearance of the first design equations. Since then different authors started investigations on Microstrip patch antennas like James Hall and David M. Pozar and there are also some who contributed a lot. Throughout the years, authors have dedicated their investigations to creating new designs or variations to the original antenna that, to some extent; produce either wider bandwidths or multiple-frequency operation in a single element. However, most of these innovations bear disadvantages related to the size, height or overall volume of the single element and the improvement in bandwidth suffers usually from a degradation of the other characteristics. It is the purpose of this thesis to introduce the general techniques produced to improve the narrow bandwidth and low frequency ratio of patch antennas.

Second most important work in this thesis is interfacing between IE3D and PSO. IE3D is a full-wave, method-of-moments based electromagnetic simulator solving the current distribution on 3D and multilayer structures of general shape. Different optimization schemes are available in IE3D, including Powell optimizer, genetic optimizer, adaptive optimizer, and random optimizer. The variables for optimization defined by IE3D are controlled by its directions and bounds. In 1995 James Kennedy and Russell Eberhart presented particle-swarm optimization (PSO), an

optimizer that models the behavior and intelligence of a swarm of bees, school of fish or flock of birds, and emphasizes both social interaction and nostalgia from the individual's perspective.

1.4 Thesis Outline

The outline of this thesis is as follows.

Chapter 2: It presents the basic theory of MSAs, including the basic geometries , feeding method and characteristics of the MSA, the advantages and disadvantages of MSAs, impedance matching, shorting techniques, the methods of analysis used for the MSA design finally The calculations needed to find the dimensions of the conventional MSA using transmission line model are presented in this chapter.

Chapter 3: In this chapter the basics of antenna parameters such as radiation pattern, impedance, VSWR, gain etc. are presented.

Chapter 4: This chapter describes the design of Single Band Rectangular Microstrip patch antenna and simulation result using the IE3D electromagnetic simulation software. The theoretical and simulation results are presented.

Chapter 5: In this chapter the Dual Frequency Operation of Microstrip antenna and the concept of dual frequency operation using the slots are described. Finally comparison between the simulation and theoretical results using IE3D.

Chapter 6: In this chapter explain the Particle Swarm Optimization algorithm and its application in antenna design.

Chapter 7: The Single and Dual Band Microstrip antenna using IE3D\PSO technique and the interfacing between the MATLAB and IE3D simulation software are

described here. Comparison between the PSO optimization result and theoretical result of Microstrip patch antenna are presented.

Chapter 8: This chapter contains conclusion and scope of future work.

CHAPTER 2

MICROSTRIP ANTENNA

2.1 Microstrip Antenna

One of the most exciting developments in antenna and electromagnetic history is the advent of Microstrip antenna (known also as patch antenna). It is probably the most versatile solution to many systems requiring planner radiating element. Microstrip antenna falls into the category of printed antennas: radiating elements that utilize printed circuit manufacturing processes to develop the feed and radiating structure. Of all the printed antennas, including dipole, slots, and tapered slots; Microstrip antenna is by far the most popular and adaptable. This is because of all its salient features: including ease of fabrication, good radiation control, and low cost of production.

The Microstrip antenna is constructed from dielectric substrate and patch metal and that a portion of the metallization layer is responsible for radiation. Microstrip antenna was conceived in the 1950s, and then extensive investigations of the patch antennas followed in the 1970s and resulted in many useful design configurations. Through decades of research, it was identified that the performance and operation of a Microstrip antenna is driven mainly by the geometry of the printed patch and the material characteristics of the substrate onto which the antenna is printed.

2.2 Basic characteristics

As shown in Figure 2.1, conventional Microstrip antennas consist of a pair of parallel conducting layers separating a dielectric medium, referred as substrate. In this configuration, the upper conducting layer or “patch” is the source of radiation where electromagnetic energy fringes off the edges of the patch and into the substrate. The lower conducting layer acts as a perfectly reflecting ground plane, bouncing energy back through the substrate and into free space. Physically, the patch is a thin conductor that is an appreciable fraction of a wavelength in extent. The patch which has resonant behavior is responsible to achieve adequate bandwidth.

Conventional patch designs yield few percent band widths. In most practical applications, patch antenna is rectangular or circular in shape; however, in general, any geometry is possible.

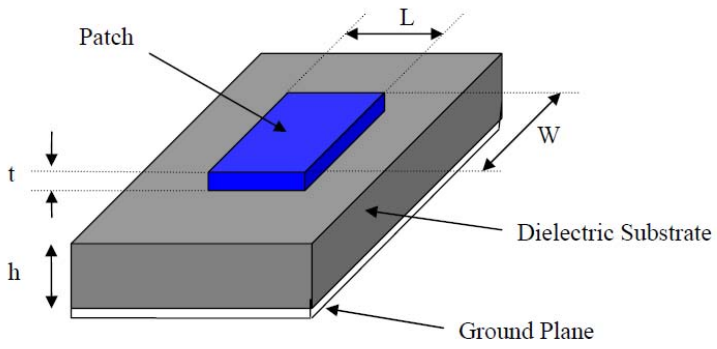

Figure 2.1Rectangular Microstrip antenna

Microstrip antenna should be designed so that its maximum wave pattern is normal to the patch. This is accomplished by proper choice of mode of excitation beneath the patch. Generally, patch of Microstrip antenna thickness is very thin in the range of t << λ_0 (λ_0 is free space wave length) and the height h of dielectric material is between $0.003\lambda_0$ < h < $0.05\lambda_0$. For a rectangular path, the length L of the element is usually λ_0 /3 < L< λ_0 /2.

There are numerous substrate that can be used for the design of Microstrip antenna, and their dielectric constants are usually in the range of 2.2< ε_r < 10, where ε_r is relative dielectric constant. The substrate whose size is thick and dielectric constant is in the range of lower end provides better efficiency and bandwidth; but it expenses large element size.

2.3 Feeding Method

There are several techniques available to feed or transmit electromagnetic energy to a microstrip antenna. The four most popular feeding methods are the Microstrip line, coaxial probe, aperture coupling and proximity coupling.

2.3.1 Coaxial Feed

The Coaxial feed or probe feed is a very common technique used for feeding Microstrip patch antennas. As seen from Figure 2.2, the inner conductor of the coaxial connector extends through the dielectric and is soldered to the radiating patch, while the outer conductor is connected to the ground plane. The main advantage of this type of feeding scheme is that the feed can be placed at any desired location inside the patch in order to match with its input impedance. This feed method is easy to fabricate and has low spurious radiation. However, its major disadvantage is that it provides narrow bandwidth and is difficult to model since a hole has to be drilled in the substrate and the connector protrudes outside the ground plane, thus not making it completely planar for thick substrates ($h > 0.02\lambda o$). Also, for thicker substrates, the increased probe length makes the input impedance more inductive, leading to matching problems [9]. It is seen above that for a thick dielectric substrate, which provides broad bandwidth, the Microstrip line feed and the coaxial feed suffer from numerous disadvantages. The non-contacting feed techniques which have been discussed below, solve these problems.

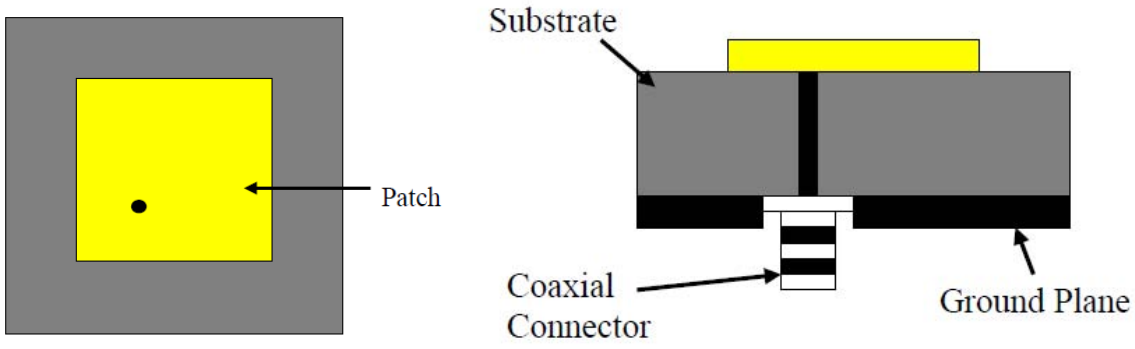

Figure 2.2 Rectangular Microstrip antenna coaxial feed

2.3.2 Microstrip Feed line

In this type of feed technique, a conducting strip is connected directly to the edge of the Microstrip patch as shown in Figure 2.3. The conducting strip is smaller in width as compared to the patch and this kind of feed arrangement has the advantage that the feed can be etched on the same substrate to provide a planar structure The purpose of the inset cut in the patch is to match the impedance of the feed line to the patch without the need for any additional matching element. This is achieved by properly controlling the inset position. Hence this is an easy feeding scheme, since it provides ease of fabrication and simplicity in modeling as well as impedance matching. However as the thickness of the dielectric substrate being used, increases, surface waves and spurious feed radiation also increases, which hampers the bandwidth of the antenna [1]. The feed radiation also leads to undesired cross polarized radiation.

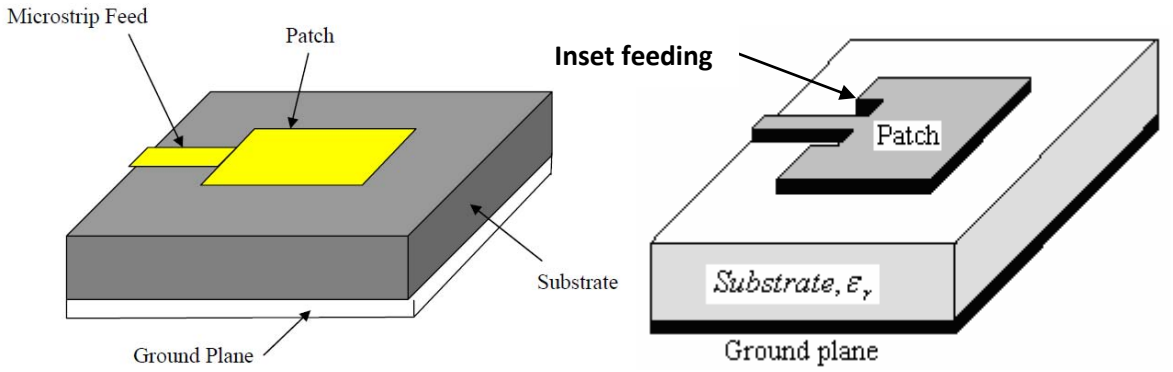

Figure 2.3 Rectangular Microstrip antenna Microstrip Line feeding

2.3.3 Aperture Coupled Feed

In this type of feed technique, the radiating patch and the Microstrip feed line are separated by the ground plane as shown in Figure 2.4. Coupling between the patch and the feed line is made through a slot or an aperture in the ground plane. The coupling aperture is usually centered

under the patch, leading to lower cross polarization due to symmetry of the configuration. The amount of coupling from the feed line to the patch is determined by the shape, size and location of the aperture. Since the ground plane separates the patch and the feed line, spurious radiation is minimized. Generally, a high dielectric material is used for the bottom substrate and a thick, low dielectric constant material is used for the top substrate to optimize radiation from the patch [1]. The major disadvantage of this feed technique is that it is difficult to fabricate due to multiple layers, which also increases the antenna thickness. This feeding scheme also provides narrow bandwidth (up to 21%).

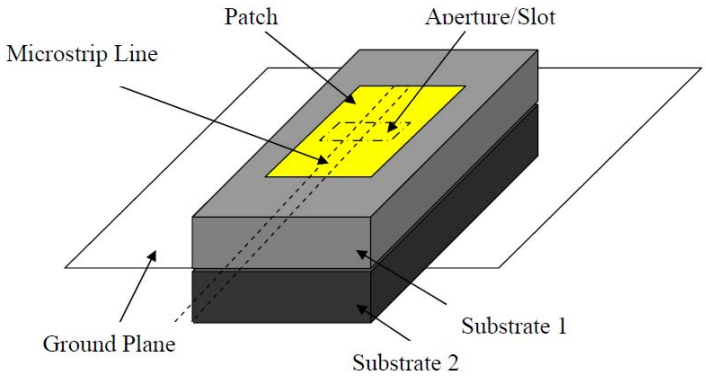

Figure 2.4 Rectangular Microstrip antenna Aperture coupled feed

2.3.4 Proximity Coupled Feed

This type of feed technique is also called as the electromagnetic coupling scheme. As shown in Figure 2.5, two dielectric substrates are used such that the feed line is between the two substrates and the radiating patch is on top of the upper substrate. The main advantage of this feed technique is that it eliminates spurious feed radiation and provides very high bandwidth (as high as 13%) [1], due to overall increase in the thickness of the microstrip patch antenna. This

scheme also provides choices between two different dielectric media, one for the patch and one for the feed line to optimize the individual performances. Matching can be achieved by controlling the length of the feed line and the width-to-line ratio of the patch. The major disadvantage of this feed scheme is that it is difficult to fabricate because of the two dielectric layers which need proper alignment. Also, there is an increase in the overall thickness of the antenna.

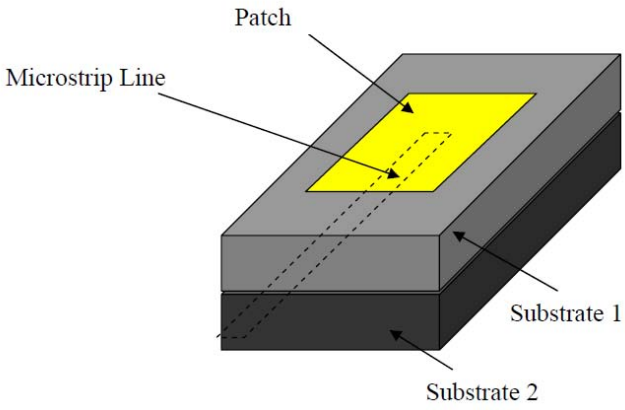

Figure 2.5 Rectangular Microstrip antenna proximity coupled feed

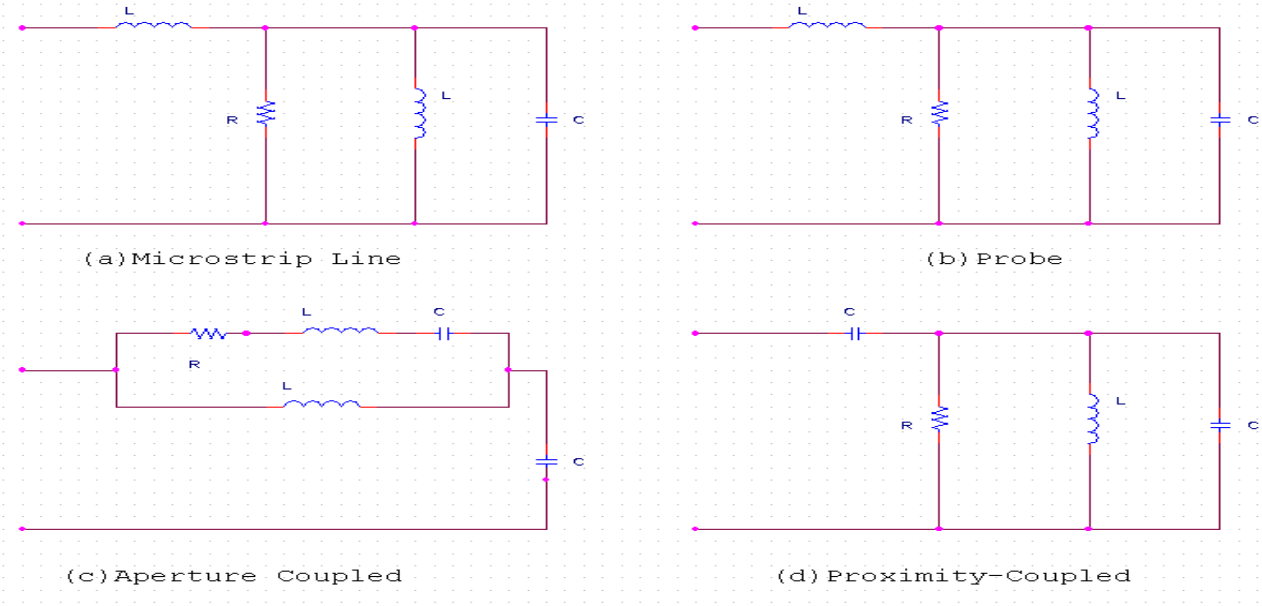

Figure 2.6 Equivalent circuits of typical feeding methods

2.4 Analytical Evaluation of a rectangular Patch Antenna

The Objectives of antenna analysis are to predict the radiation characteristics such as radiation patterns, gain, and polarization as well as input impedance, bandwidth, mutual coupling, and antenna efficiency. The analysis of microstrip antennas is complicated by the presence of in homogeneity of dielectric and boundary conditions, narrow frequency band characteristics, and a wide variety of feed, patch shape, and substrate configurations. The good model has the following basic characteristics:

- It can be used to calculate all impedance and radiation characteristics of the antenna
- Its results are accurate enough for the intended purpose
- It is simple and possible, while providing the proposed accuracy for the impedance and radiation properties.
- It lends itself to interpretation in terms of known physical phenomena.

In common practice, microstrip antennas are evaluated using one of three analysis methods: the transmission line model, the cavity model, and the full-wave model. The transmission line model is the easiest of all, it gives good physical insight. But it is less accurate and more difficult to model coupling effect of antenna. Compared to the transmission line model, the cavity model is more accurate but at the same time more complex and difficult to model coupling effect. In general, when applied properly, the full wave model is very accurate, and very versatile.

It can analyze single element, finite array, layered elements and arbitrary shaped element of microstrip antenna and also coupling effect of the antenna.

2.4.1 Transmission line modeling

The transmission line model, as shown in the Figure 2.4, represents the microstrip antenna by two slots, separated by susceptance B and conductance G of length L patch. Due to the dimensions of the patch are finite (or shorter than the base plate) along in length and width, the fields at the edges of the patch undergo fringing. The fringing fields act to extend the effective length of the patch. Thus, the length of a half-wave patch is slightly less than a half wavelength in the dielectric material.

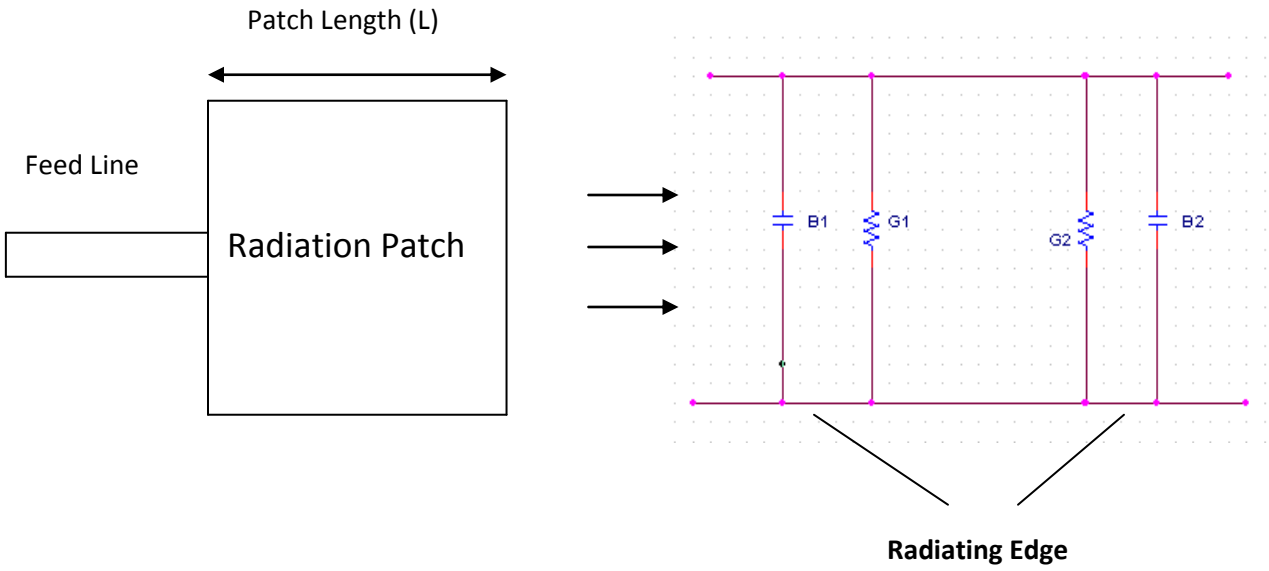

Figure 2.7 Transmission line model

2.4.1.1 Fringing Effect

The amount of fringing of the antenna is a function of the dimensions of the patch and the height of the substrate. Due to fringing electric field lines travels in non-homogeneous material, typically substrate and air, an effective dielectric constant ε_{reff} is introduced. For electric line with air above the substrate, the effective dielectric constant has values in the range of

$1 < \varepsilon_{reff} < \varepsilon_r$. The dielectric constant for most applications is much greater than unity. The effective dielectric constant is expressed by the function of frequency. As the frequency of operation increases, most of the electric field concentrates in the substrate, and therefore, the microstrip behaves more like a homogeneous electric line of one dielectric, and the effective dielectric constant approaches the value of one dielectric constant of the substrate. Experimental results of the effective dielectric constant for microstrip with three different substrates are shown in Figure 2.8

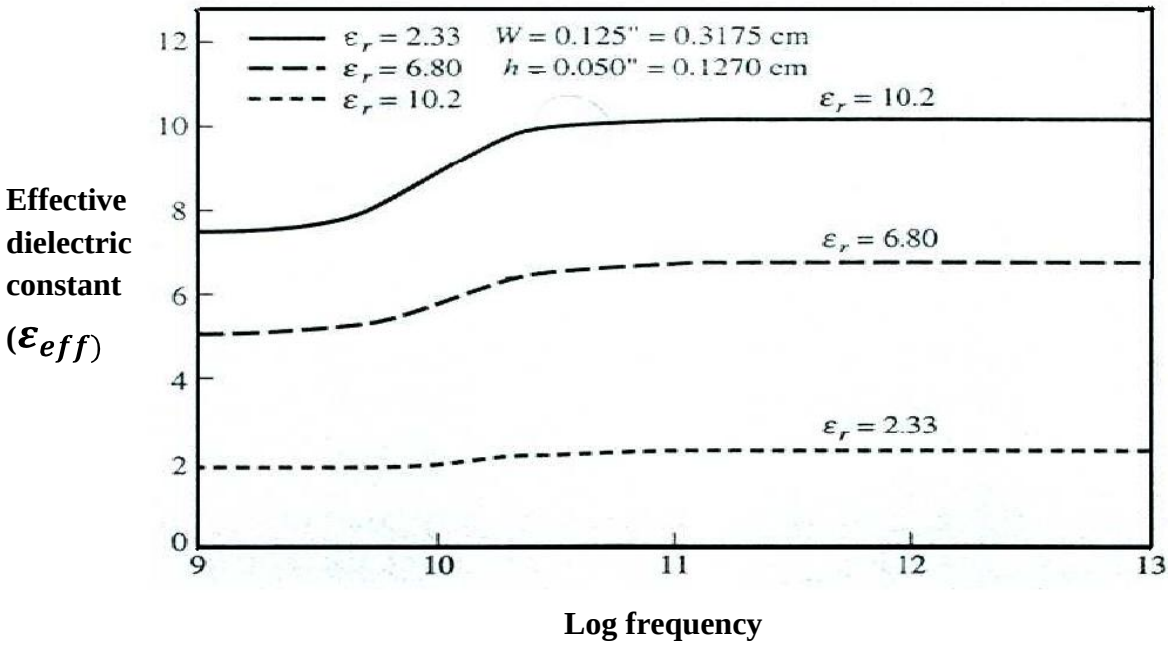

Figure 2.8 Effective dielectric constant versus frequency for typical substrates

Generally, the relationship of width (W) height (h) effective dielectric constant, (ε_{eff}) and relative

dielectric constant of the substrate (ε_r) are related as follow [4][15]

$$\varepsilon_r = \frac{\varepsilon_r + 1}{2} + \frac{\varepsilon_r - 1}{2}\left[\frac{1}{\sqrt{1 + 12\left(\frac{h}{W}\right)}}\right] \qquad (2.1)$$

A very popular and practical approximation relation for normalized extension of the length is obtained from below equation. [5][15].

$$\Delta L = 0.412h\frac{(\varepsilon_r + 0.3)(\frac{W}{h} + 0.264)}{(\varepsilon_{eff} - 0.258)(\frac{W}{h} + 8)} \qquad (2.2)$$

Substrate thickness should be chosen as large as possible to maximize bandwidth, but not so large to minimize the risk of surface wave excitation. The substrate should also has low dielectric constant in order to achieve high efficiency.

Since the effective length of the patch has been extended by ΔL on each side, the effective length of the patch is expressed as

$$L_{eff} = L + 2\Delta L \qquad (2.3)$$

After analyzing and determining the physical nature of the Microstrip antenna with reference of resonant frequency, f_r , relative dielectric constant, ε_r , height of the substrate h; it is possible to design rectangular microstrip antenna dimension, width *W* and Length *L* , of patch as follow. [6]

$$W = \frac{\lambda_o}{2}((\varepsilon_r + 1)/2)^{-\frac{1}{2}} \qquad (2.4)$$

$$L = \frac{1}{2f_r\sqrt{\varepsilon_{eff}}\sqrt{\mu_0\varepsilon_0}} - 2\Delta L \qquad (2.5)$$

2.4.1.2 Resonant Input Resistance

As shown in figure 2.4, a Microstrip antenna is represented by an equivalent circuit with two slots having conductance, G, and susceptance, B. The total admittance at slot one (input

admittance) is obtained by transferring the admittance of slot two from the output terminal to input terminals using the admittance transformation equation of transmission lines. Ideally two slots are separated by λ /2 where λ is the wavelength in the dielectric (substrate). However, because of the fringing the length of the patch is electrically longer than the actual length. Therefore the actual separation of the two slots is slightly less than λ/2. If the reduction of the length is properly chosen using equation 2.2, the transformed admittance of the slot two becomes.

$$Y_1=Y_2 \qquad G_1=G_2 \qquad B_1=-B_2 \tag{2.6}$$

Therefore the total resonant input admittance is real and is given by:-

$$Y_{in}=Y_1+Y_2=2G_1 \tag{2.7}$$

Since the total input admittance is real, the resonant input impedance is also real.

$$Z_{in} = \frac{1}{Y_{in}} = R_{in} = \frac{1}{2G_1} \tag{2.8}$$

Considering the mutual effects between the slots, the above equation will be modified as [13]

$$R_{in} = \frac{1}{2(G_1 \pm G_{12})} \tag{2.9}$$

where the plus (+) sign is used for modes with odd (anti-symmetric) resonant voltage distribution beneath the patch and the slots while minus (-) sign is used for modes with even (symmetric) resonant voltage distribution.

However, the mutual conductance of Microstrip antenna is defined as [1]

$$G_{12} = \frac{1}{|V_0|} Re \iint_S E_1 x H_2^* . ds \tag{2.10}$$

where E_1 is the electric field radiated by slot one, H_2 is the magnetic field radiated by slot two, V_0 is the voltage across the slot.

The equation (2.12) considers the effect of magnetic field radiated by slot two over slot one of the equivalent circuit of microstrip antenna. The integration is performed over the sphere of large radius.

Hence, G_{12} can also be calculated using [14]

$$G_{12} = \frac{1}{120\pi^2}\int_0^{\pi}\left[\sin\left[\frac{k_o w cos\theta}{2}\right]/cos\theta\right]^2 J_o(k_o L sin\theta)\sin^3\theta d\theta \qquad (2.11)$$

Where J_0 is the Bessel function of the first kind of order zero and K_0 is a wave number

However, the conductance, G_1, is obtained from radiated power expression: [1]

$$G_1 = \frac{2P_{rad}}{|V|^2} \qquad (2.12)$$

Where p_{rad} is the radiated power of Microstrip antenna [1] given as

$$P_{rad} = \frac{|V_o|^2}{2\pi\eta_o}\int_0^{\pi}\left[\sin\left(\frac{k_o w cos\theta}{2}\right)/cos\theta\right]^2 \sin^3\theta d\theta \qquad (2.13)$$

Therefore the conductance can be expressed as

$$G_1 = \frac{I_1}{120\pi^2} \qquad (2.14)$$

Where

$$I_1 = \int_0^{\pi}\left[\sin\left(\frac{k_o w cos\theta}{2}\right)/cos\theta\right]^2 \sin^3\theta d\theta \qquad (2.15\ a)$$

The approximated result of equation 2.15.a is [1]

$$I_1 = -2 + \cos(X) + XS_i(X) + \frac{\sin(X)}{X} \qquad (2.15\ b)$$

$$X = k_o W \qquad (2.15\ c)$$

And hence, asymptotic value of the equation is described by [1]

$$G_1 = \frac{1}{90}\left(\frac{W}{\lambda_o}\right) \qquad (2.16)$$

$$G_1 = \frac{1}{120}\left(\frac{W}{\lambda_o}\right)$$

Graphical representation of equation 2.16 to determine G1 is presented in the Figure 2.6 (A plot of G1 as a function of W/λ_0). It shows that magnitude of conductance of the Microstrip antenna increases linearly as W/λ_0 increases .

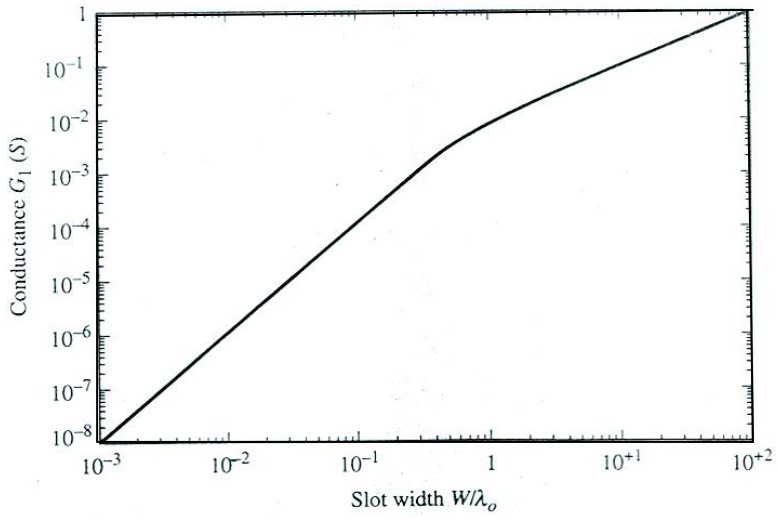

Figure 2.9 Slot conductance as a function of slot width [1]

2.4.1.3 Inset Feed

The resonant input resistance of the Microstrip antenna obtained by equation 2.11 can be changed to appropriate value using inset feed or other alternative technique in order to achieve maximum power transfer.

The inset technique changes the resonant input resistance by introducing a physical notch, as shown in Figure 2.10, which in turn introduces a junction capacitance. The physical notch and its corresponding junction capacitance influence slightly the resonant frequency. The maximum

resonant input resistance value occurs at the edge of the slot (y_0 = 0) where the voltage is maximum and current is minimum. However, the minimum resonant input resistance value occurs at the center of the patch (y_0 = L/2). As the inset feed point moves from edge toward the center of the patch the resonant input impedance decreases monotonically and reaches zero at the center. When the value of the inset feed-point reaches the center of the patch (y_0 = L/2), the $cos^2(\frac{\pi}{L}y_0)$ function varies very rapidly; therefore the input resistance also changes rapidly with the position of the feed point.

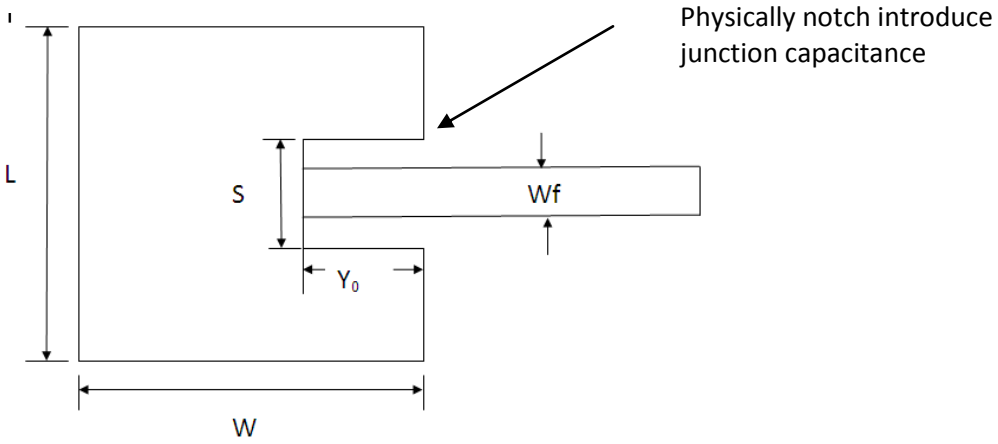

Figure 2.10 (a) Microstrip line inset feeding

Maximum resonant input resistance at the

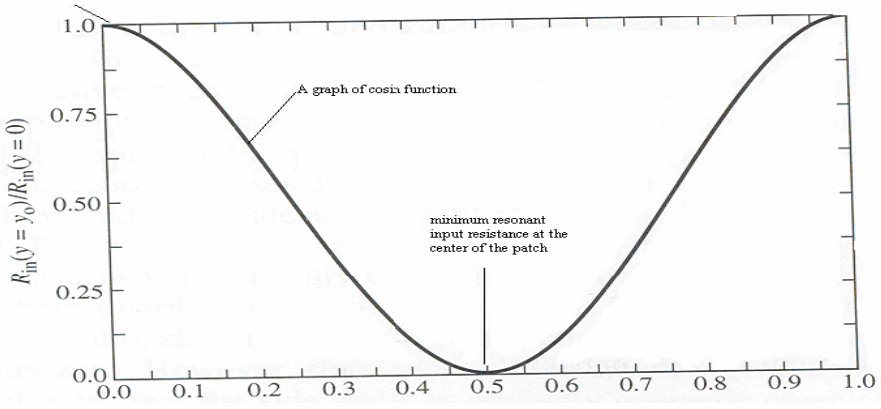

Figure 2.10 (b) variation of normalized input resistance

Analytically, the input resistance for inset feed is given approximately by [1] & [16]

$$R_{in}(y=0) = \frac{1}{G_1 \pm G_{12}} cos^2\left(\frac{\pi}{L} y_0\right) \qquad (2.17)$$

Similarly the characteristics impedance Z_0 of Microstrip line feed is given by [4]

$$Z_c = \frac{60}{\sqrt{\varepsilon_{reff}}} ln\left[\frac{8h}{W_0} + \frac{W_0}{4h}\right] \qquad \frac{W_0}{4h} \leq 1 \qquad (2.18)$$

$$Z_c = \frac{120\pi}{\sqrt{\varepsilon_{reff}}\left[\frac{W_o}{h} + 1.393 + 0.667 ln\left(\frac{W_o}{h} + 1.44\right)\right]} \qquad \frac{W_0}{4h} \geq 1$$

Characteristic impedance of Microstrip line as function w/h is given in Figure 2.11 for common substrates such as RT (2.33), beryillium oxide (6.8) and alumina (10.2). As it is indicated in the Figure 2.11 the characteristic impedance Z_0 is decreased as w/h values increased. For instance, the characteristic impedance 50 ohm is obtained for RT (2.33) dielectric material at the ratio value of w/h of $10^{0.5}$.

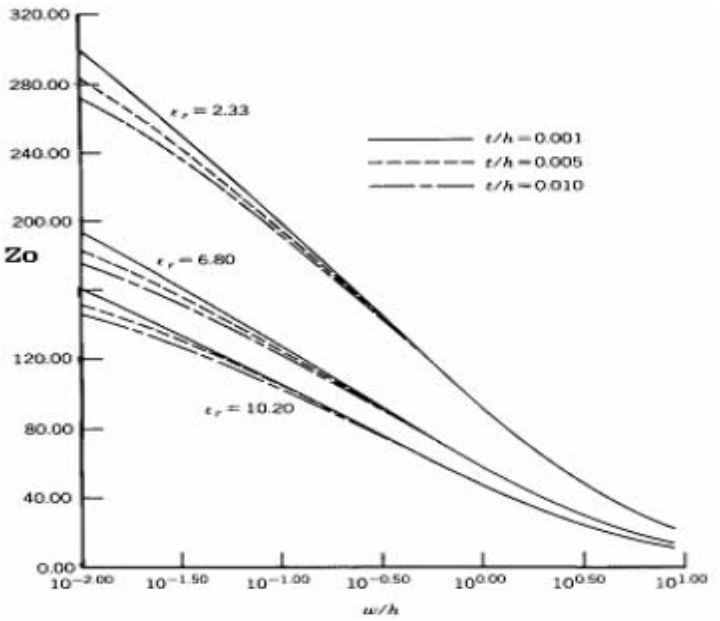

Figure 2.11 Characteristics impedance of Microstrip line as a function of w/h

2.4.2 The Cavity Model

Microstrip antenna resembles dielectric loaded cavities, and exhibit higher order resonances. The normalized fields within the dielectric substrate can be found more accurately by treating that region as a cavity bounded by electric conductors (above and below) and by magnetic wall along the perimeter of the patch. The bases for this assumption are the following points (for height of substrate h << wave length of the field λ).

- The fields in the interior region do not vary with z-axis because the substrate is very thin, h<< λ.
- The electric field is z-axis directed only, and the magnetic field has only the transverse components in the region bounded by the patch metallization and the ground plane. This observation provides for the electric walls at the top and bottom.
- The electric current in the patch has no component normal to the edge of the patch metallization, which implies that the tangential component of magnetic field along the edge is negligible, and a magnetic wall can be placed along the periphery.

This approximation model leads to reactive input impedance, and it does not radiate any power. However, the actual fields can be approximated to the generated field of the model and is possible to analyze radiation pattern, input admittance, and resonant frequency.

2.4.2.1 Current Densities

When the Microstrip antenna (cavity modeled) is energized, charge distribution is established on upper and lower surfaces of the patch, as well as on the surface of the ground plane. The charge distribution is controlled by two mechanisms; attractive and a repulsive mechanism. The attraction is between the corresponding opposite charges on the

bottom side of the patch and ground plane, which tends to maintain the charge concentration on the bottom of the patch. The repulsive is between like charges from the bottom of the patch, around its edges, to its top surface as shown in Figure 2.12. The movement of these charges creates corresponding current densities J_b and J_t , at the bottom and top surfaces of the patch.

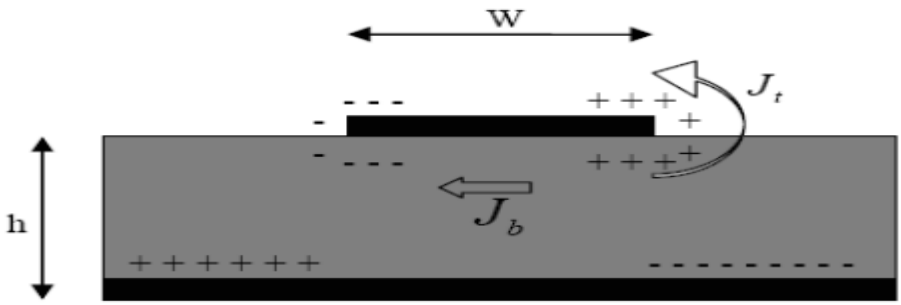

Figure 2.12 charge distribution and current density

Since for the most practical microstrip the height to width ratio is very small, and due to attractive and a repulsive mechanism of charges, only small amount of current flows at the top surface of the patch and large amount of charges are concentrated underneath the patch. The concentration of charges produces current density J_b and J_t at the patch. However, this flow of current decrease as the height to width ratio increases. It implies that there is no tangential magnetic field component at the edges of the patch. This condition allows a Microstrip antenna to be modeled by a four sided magnetic wall (Figure 2.13) model as shown in Figure 2.13.

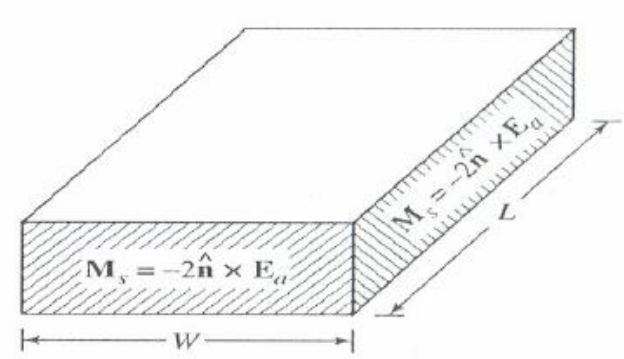

Figure 2.13 Cavity model of rectangular Microstrip antenna

As shown in the Figure 2.13, the four sides slot is represented by the equivalent electric current density and equivalent magnetic current densities, respectively as follows.

$$J_s = nxH_a \qquad and \qquad M_s = -nxE_a \tag{2.19}$$

Where E_a and H_a represent the electric and the magnetic field at the slots.

Considering the presence of the ground plane, the only nonzero current density is the equivalent magnetic current density M_s.

Applying image theory of the magnetic current in the electric ground plane, equivalent magnetic current density M_s is given as

$$M_s = -2nxE_a \tag{2.20}$$

Typical E and H plane of Microstrip antenna of two slots with the source of the same magnitude and phase is presented in Figure 2.14.

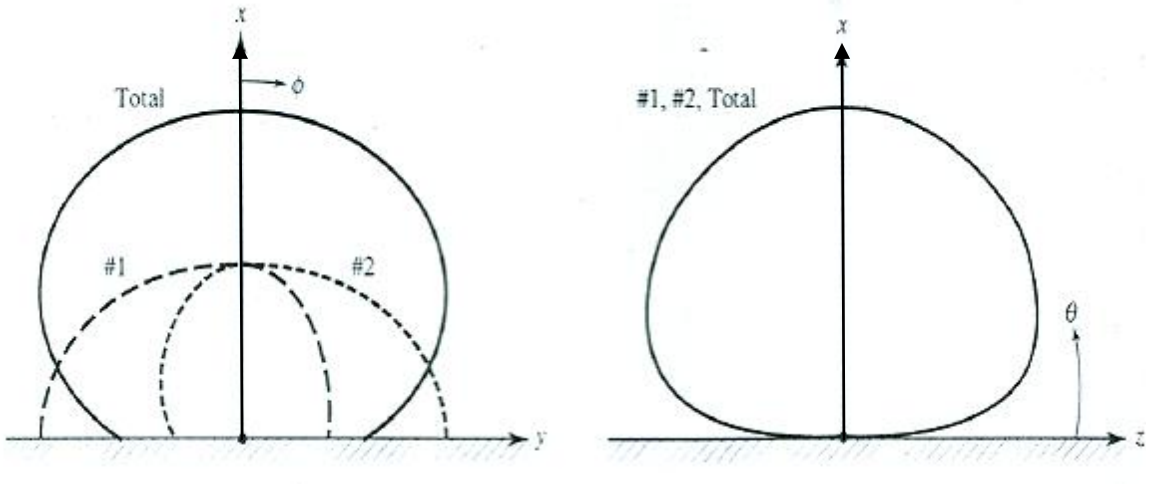

(a) E-Plane **(b) H-Plane**

Figure 2.14 Typical E and H plane of microstrip patch antenna

Treating the cavity model as Microstrip antenna is not sufficient to find the absolute amplitude of the electric and magnetic fields. Naturally, the cavity is lossless and requires introducing losses by considering effective loss tangent to behave as an antenna. Because the thickness of the microstrip antenna is usually very small, the waves generated within the dielectric substrate undergo considerable reflections when the fields arrive at the edge of the patch. The electric field is nearly normal to the surface of the patch. Therefore, only TM field configuration is considered within the cavity.

2.4.2.2 Field Configuration

It is common practice in the analysis of electromagnetic boundary-value problems to use auxiliary vector potentials as aids in obtaining solution for electric (**E**) and magnetic (**H**) fields. The most common vector potential functions are the **A**, Magnetic vector potential, and **F**, electric vector potential. These field configurations must be satisfy Maxwell's equations or the wave equation and the appropriate boundary conditions.

Transverse magnetic modes, (TM) are field configurations whose magnetic field components lie in a plane that is transverse to the direction of wave propagation. Consider that the wave propagation of the microstrip antenna is to x-axis and hence, magnetic vector potential of cavity model is generally obtained from the homogeneous wave equation [4] & [8].

$$\nabla^2 A_x + k^2 A_x = 0 \qquad (2.21)$$

Where $k^2 = \omega^2 \mu\varepsilon$

Since the field expression of TM to a given direction is independent of the other coordinate system, it is sufficient to let the vector potential **A** have only a component in the direction in which the fields are propagated. The remaining components of **A** as well as all of **F** are set equal to zero.

The solution for equation 2.21 is expressed as follow [4]:

$$A_x = [A_1 \cos(k_x x) + B_1 sink_x x]\left[A_2 \cos\left(k_y y\right) + B_2 sink_y y\right][A_x \cos(k_z z) + B_x sink_z z] \quad (2.22)$$

Wherek_x, k_y and k_z are the wave numbers along x, y, z directions, respectively. Its value is determined subject to the boundary conditions.

Considering the boundary condition of the cavity model, H_z(0<x<h, y=0, 0<z<W)= 0 and H_z (0<x<h, y=L,0<z<W)=0, the vector potential is described as

$$A_x = A_{mnp} \cos(k_x x') \cos\left(k_y y'\right) \cos(k_z z') \qquad (2.23)$$

Where A_{mnp} represents the amplitude coefficients of each *mnp* mode

Resonant frequency determines the dominant mode of cavity operation and it is obtained using the following equations [4] & [1].

1. If L>W>h, the mode with lowest frequency (dominant mode) is TM_{010} and its resonant frequency is:

$$(f_r)_{010} = \frac{1}{2L\sqrt{\mu\varepsilon}} \qquad (2.24)$$

2. If L>W>L/2, the mode is TM_{001} and its resonant frequency is:

$$(f_r)_{001} = \frac{1}{2L\sqrt{\mu\varepsilon}} \qquad (2.25)$$

3. If L>L/2>W>h, the order of the mode is TM_{020} and its resonant frequency is:

$$(f_r)_{020} = \frac{1}{2L\sqrt{\mu\varepsilon}} \qquad (2.26)$$

CHAPTER 3

ANTENNA PARAMETERS

3.1 Gain and directivity

The gain of an antenna is the radiation intensity in a given direction divided by the radiation intensity that would be obtained if the antenna radiated all of the power delivered equally to all directions. The definition of gain requires the concept of an isotropic radiator; that is, one that radiates the same power in all directions. An isotropic antenna, however, is just a concept, because all practical antennas must have some directional properties. Nevertheless, the isotropic antenna is very important as a reference. It has a gain of unity (g = 1 or G = 0 dB) in all directions, since all of the power delivered to it is radiated equally well in all directions.

Although the isotopes are a fundamental reference for antenna gain, another commonly used reference is the dipole. In this case the gain of an ideal (lossless) half wavelength dipole is used. Its gain is 1.64 (G = 2.15 dB) relative to an isotropic radiator.

The gain of an antenna is usually expressed in decibels (dB). When the gain is referenced to the isotropic radiator, the units are expressed as dBi; but when referenced to the half-wave dipole, the units are expressed as dBd. The relationship between these units is

$$G_{dBd}G_{dBd} = G_{dBi}G_{dBi} - 2.15\ \text{dBidB} \qquad (3.1)$$

Directivity is the same as gain, but with one difference. It does not include the effects of power lost (inefficiency) in the antenna. If an antenna were lossless (100 % efficient), then the gain and directivity (in a given direction) would be the same.

3.2 Antenna Polarization

The term polarization has several meanings. In a strict sense, it is the orientation of the electric field vector E at some point in space. If the E-field vector retains its orientation at each point in space, then the polarization is linear; if it rotates as the wave travels in space, then the polarization is circular or elliptical. In most cases, the radiated-wave polarization is linear and either vertical or horizontal. At sufficiently large distances from an antenna, beyond 10 wavelengths, the radiated, far-field wave is a plane wave.

3.3 Input impedance

There are three different kinds of impedance relevant to antennas. One is the terminal impedance of the antenna, another is the characteristic impedance of a transmission line, and the third is wave impedance. Terminal impedance is defined as the ratio of voltage to current at the connections of the antenna (the point where the transmission line is connected). The complex form of Ohm's law defines impedance as the ratio of voltage across a device to the current flowing through it.

The most efficient coupling of energy between an antenna and its transmission line occurs when the characteristic impedance of the transmission line and the terminal impedance of the antenna are the same and have no reactive component. When this is the case, the antenna is considered to be matched to the line. Matching usually requires that the antenna be designed so that it has a terminal impedance of about 50 ohms or 75 ohms to match the common values of available coaxial cable.

The input impedance of patch antenna is in general complex and it includes resonant and non-resonant part. Both real and imaginary parts of the impedance vary as a function of frequency. Ideally, both the resistance and reactance exhibit symmetry about the resonant

frequency as shown in Figure 3.1. Typically, the feed reactance is very small, compared to the resonant resistance for thin substrates.

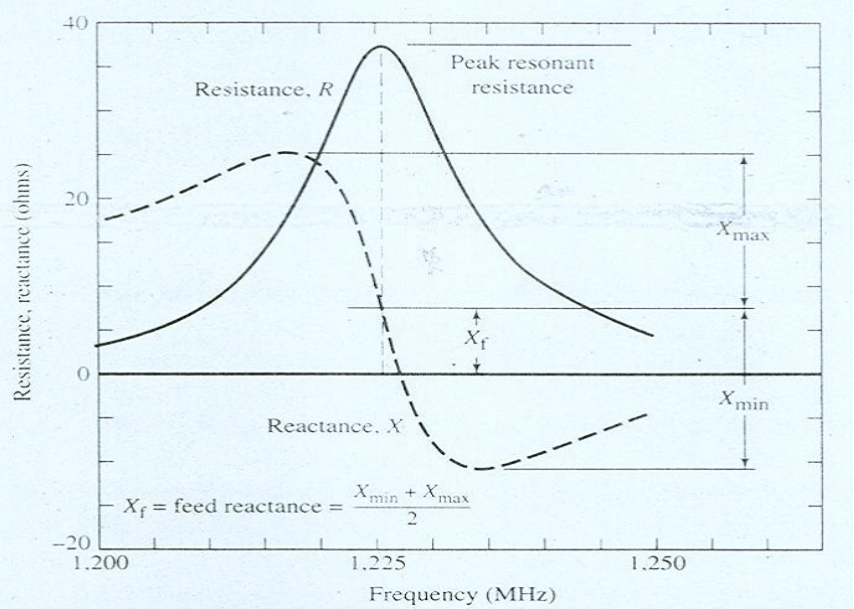

Figure 3.1 *Typical variation of resistance and reactance of rectangular Microstrip antenna versus frequency*

3.4 Voltage Standing Wave Ratio

The standing wave ratio (SWR), also known as the voltage standing wave ratio (VSWR), is not strictly an antenna characteristic, but is used to describe the performance of an antenna when attached to a transmission line. It is a measure of how well the antenna terminal impedance is matched to the characteristic impedance of the transmission line. Specifically, the VSWR is the ratio of the maximum to the minimum RF voltage along the transmission line. The maxima and minima along the lines are caused by partial reinforcement and cancellation of a forward moving RF signal on the transmission line and its reflection from the antenna terminals.

If the antenna terminal impedance exhibits no reactive (imaginary) part and the resistive (real) part is equal to the characteristic impedance of the transmission line, then the antenna and

transmission line are said to be matched. It indicates that none of the RF signal sent to the antenna will be reflected at its terminals. There is no standing wave on the transmission line and the VSWR has a value of one. However, if the antenna and transmission line are not matched, then some fraction of the RF signal sent to the antenna is reflected back along the transmission line. This causes a standing wave, characterized by maxima and minima, to exist on the line. In this case, the VSWR has a value greater than one. The VSWR is easily measured with a device and VSWR of 1.5 is considered excellent, while values of 1.5 to 2.0 is considered good, and values higher than 2.0 may be unacceptable.

3.5 Bandwidth

The bandwidth of an antenna is defined as the range of frequency within the performance of the antenna. In other words, characteristics of antenna (gain, radiation pattern, terminal impedance) have acceptable values within the bandwidth limits. For most antennas, gain and radiation pattern do not change as rapidly with frequency as the terminal impedance does. Since the transmission line characteristic impedance hardly changes with frequency, VSWR is a useful, practical way to describe the effects of terminal impedance and to specify an antenna's bandwidth.

For broadband antennas, the bandwidth is usually expressed as the ratio of the upper to lower frequencies of acceptable operation. However, for narrowband antennas, the bandwidth is expressed as a percentage of the bandwidth. [1]

3.6 Quality factor

The quality factor is a figure-of-merit that representative of the antenna losses. Typically there are radiation, conduction, dielectric and surface wave losses.

$$\frac{1}{Q_t} = \frac{1}{Q_{rad}} + \frac{1}{Q_c} + \frac{1}{Q_d} + \frac{1}{Q_{sc}} \quad (3.2)$$

Q_t : Total quality of factor

Q_{rad}: Quality factor due to radiation losses

Q_c : Quality factor due to conduction losses

Q_{dm}: Quality factor due to dielectric losses

Q_{sc}: Quality factor due to surface wave

The quality factor, bandwidth and efficiency are antenna figures-of-merit, which are interrelated, and there is no complete freedom to independently optimize each one.

For very thin substrates h << λ_0 of arbitrary shapes including rectangular, there approximate formulas to represent the quality factors of the various losses.

These can be expressed as

$$Qc = h\sqrt{\pi f \mu \sigma} \quad (3.3)$$

$$\mathrm{Q_d} = \frac{1}{\tan \delta \delta} \quad (3.4)$$

$$Q_{rad} = \frac{2\omega\varepsilon}{hG_t/_l} \quad (3.5)$$

Where tan δ is the loss tangent of the substrate material, σ is the conductivity of the conductors associated with the patch and ground plane, G_t/l is the total conductance per unit length of the radiating aperture and k for rectangular microstrip antenna is $L/4$.

The Q_{rad} as represented by 3.5 is inversely proportional to the height of the substrates. A typical variation of the bandwidth for a Microstrip antenna as a function of the normalized height of the substrate, for two different substrates, is shown in Figure 3.1. It is evident that the

bandwidth increases as the substrate height increases. However, the radiation efficiency of the patch antenna described by the ratio of power radiated over the input power (3.6) decreases as normalized height of the substrate increased.

$$\eta = \frac{Q_t}{Q_{rad}} \qquad (3.6)$$

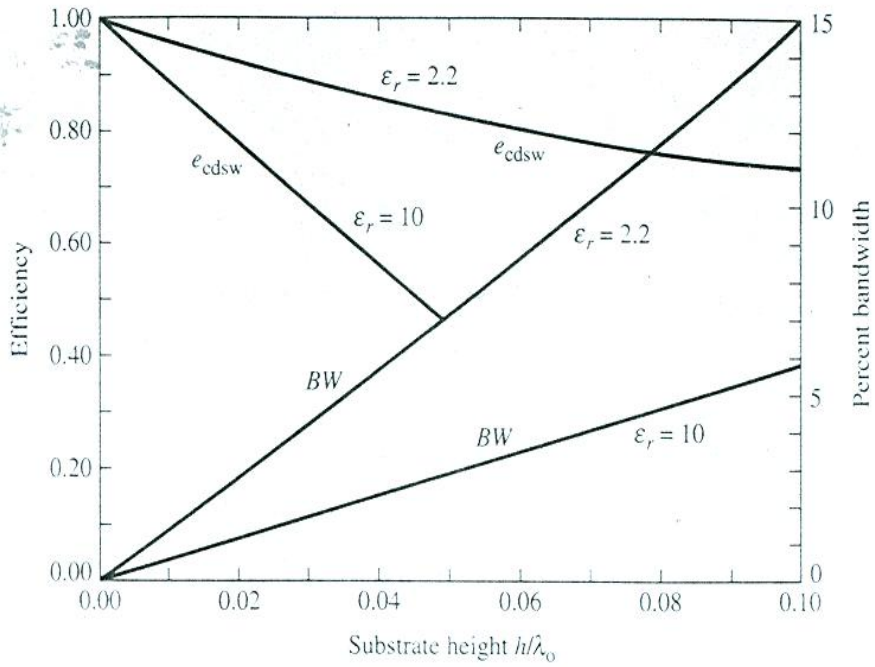

Figure 3.2 Efficiency and bandwidth versus substrate height at constant resonant frequency for Rectangular Microstrip patch for two different substrates [19]

CHAPTER 4

SINGLE BAND MICROSTRIP ANTENNA

4.1 Rectangular Microstrip Antenna

The rectangular patch antenna is approximately a one-half wavelength long section of rectangular Microstrip transmission line. When air is the antenna substrate, the length of the rectangular Microstrip antenna is approximately one-half of a free-space wavelength. As the antenna is loaded with a dielectric as its substrate, the length of the antenna decreases as the relative dielectric constant of the substrate increases. The resonant length of the antenna is slightly shorter because of the extended electric "fringing fields" which increase the electrical length of the antenna slightly. This is we explained in chapter 1 in previous.

4.2 Single Band Microstrip Antenna

A single element of rectangular patch antenna, as shown in Figure 4.1, can be designed for the 2.4 GHz resonant frequency using transmission line model taking eqn. 2.4, 2.5, 2.13 and 2.20.

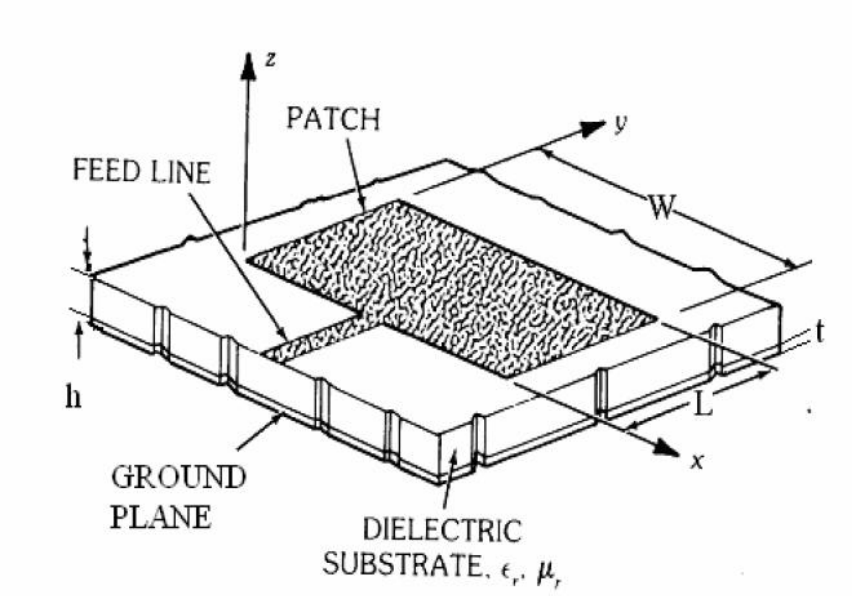

Figure 4.1Typical Rectangular Patch Antenna

In the typical design procedure of the Microstrip antenna, the desired resonant frequency, thickness and dielectric constant of the substrate are known or selected initially. In this design of rectangular Microstrip

antenna, a RT Duriod dielectric material ($\varepsilon_r = 2.4$) with dielectric loss tangent $\tan\delta$ of 0.001 is selected as the substrate with 1.58 mm height[7]. Then, a patch antenna that operates at the specified operating frequency f0 = 2.4 GHz can be designed by the following steps using transmission line model equations. The antenna is existed by the INSET feed away from the center of the patch.

The essential parameter specifications for the design of the rectangular microstrip patch antenna are as in Table 4.1.

Shape	**Single Band Rectangular**
Frequency of operation	2.4 GHz
Dielectric constant of substrate	2.4 (RT Duriod)
Height of the dielectric substrate	1.58 mm
Feeding method	INSET feeding
VSWR	1.5:1
Beamwidth Azimuth Zenith	 <100 <100
Gain	5 dBi - 8dBi
Polarization	Linear

Table 4.1 Design parameter specifications of microstrip antenna.

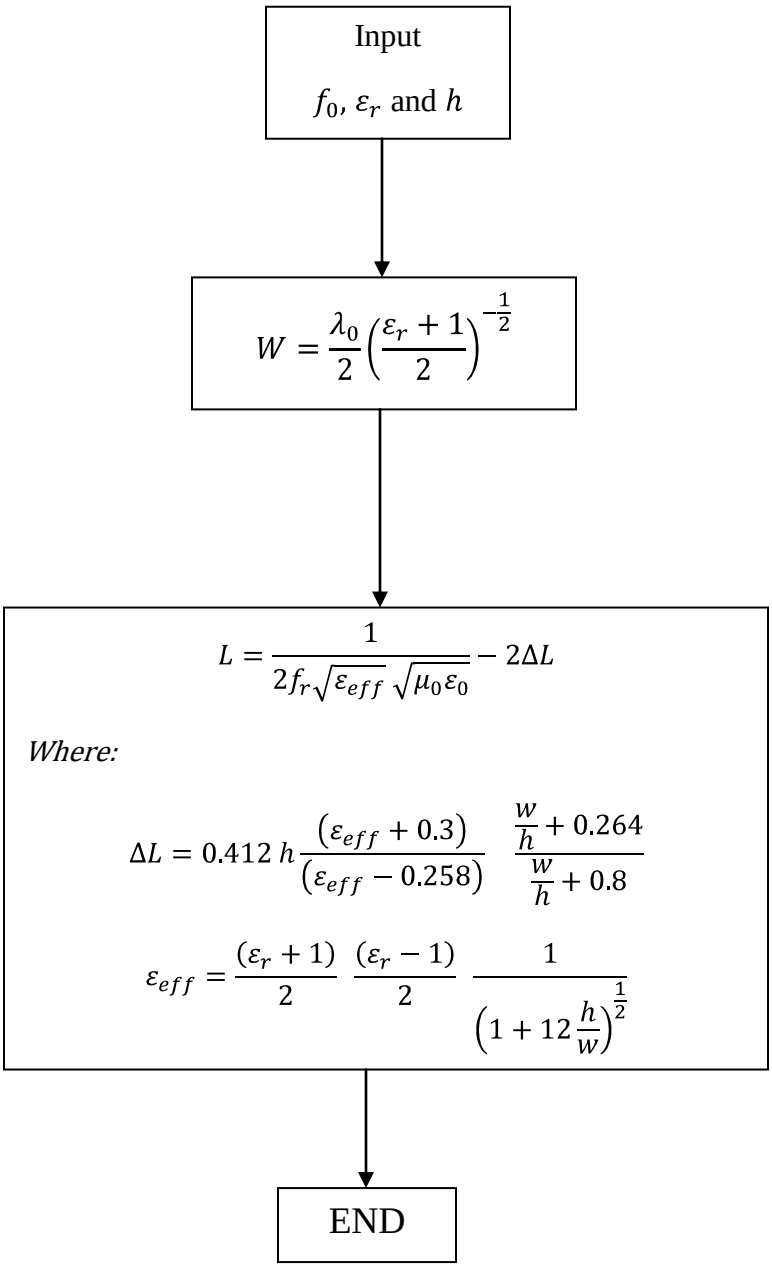

Figure 4.2 Flow chart based on usual design procedure for rectangular patch antenna

Steps required for calculating width (W) and Length (L) of microstrip antenna

- **Step 1**. Initially, select the desired resonant frequency, thickness and dielectric constant of the substrate.
- **Step 2**. Obtain Width(W) of the patch by inserting ε_r *and* λ_0

- **Step 3**. Obtain Length (L) of the patch after determining $\Delta L \; and \; \varepsilon_r$.

It is also possible to determine the inset length of the patch to ensure matching from the flow chart (Figure 4.7) taking the resonant wave length λ_0 , width W and length L of the patch as input.

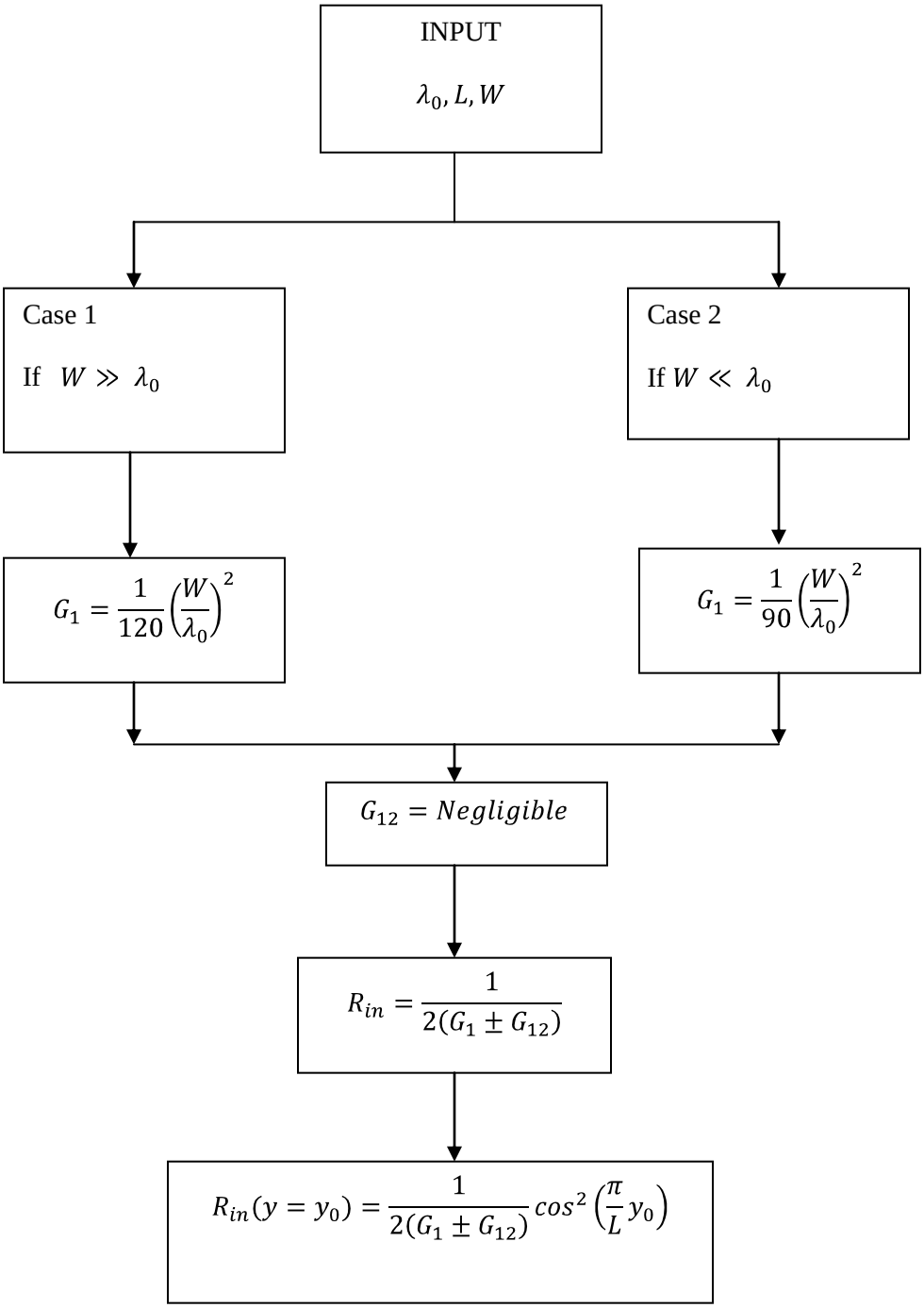

Figure 4.3 Flow chart to determine the inset length of the patch

Steps required for calculating the inset depth of single band Microstrip patch antenna

- **Step 1**: Consider that L, W of the patch is calculated and λ_0 is known. (As an input)
- **Step 2**: Depending to magnitude of W greater or less than λ_0; and then determine G1.
- **Step 3**: Assume that G12 is negligible and fined input resistance of the patch.
- **Step 4**: Consider that the characteristic impedance of Microstrip line feeder is 50 ohm. Thus, equate the equation to obtain matching between the input impedance of the patch and feeder. (i.e. inset length, y_0).

Calculation result of Microstrip patch antenna shown in table 4.2

Result:

Design of Single Band Microstrip Patch Antenna	
Width of the Patch(W)	46.9 mm
Effective dielectric constant of the Patch,(ε_{eff})	2.2922
Length of the Patch(L)	39.6 mm
Input Resistance of the Patch(R_{in})	50 Ω
Inset Depth of the Patch(y_0)	13 mm
Width of Microstrip line (w_0)	4.2 mm

Table 4.2 Calculated result of single band rectangular microstrip antenna

4.3 Geometry of Proposed Antenna

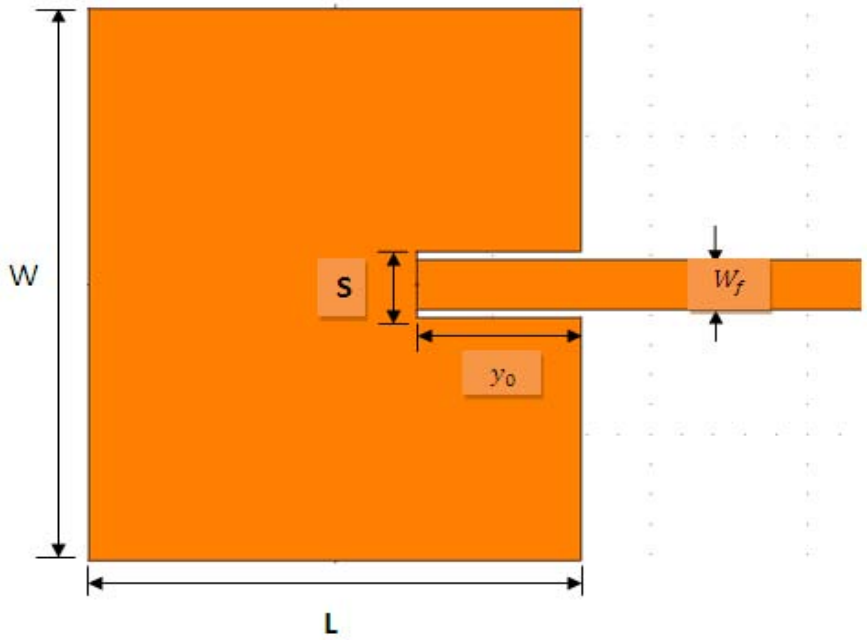

Figure 4.4 Geometry of Single Band Microstrip Antenna

4.4 Simulation Setup and Result

4.4.1 Simulation Setup

The software used to model and simulate the Microstrip patch antenna is Zeland Inc's IE3D. IE3D is a full-wave electromagnetic simulator based on the method of moments. It analyzes 3D and multilayer structures of general shapes. It has been widely used in the design of MICs, RFICs, patch antennas, wire antennas, and other RF/wireless antennas. It can be used to calculate and Return loss plot, VSWR, current distributions, radiation patterns etc. For design simplicity of the conventional MSA, the patch's length and width are shows in the table 4.2.

4.4.2 Return loss and Antenna Bandwidth

The Inset feed used to design the rectangular patch antenna. The center frequency is selected as the one at which the return loss is minimum. As described in chapter two, the bandwidth can be calculated from the return loss (RL) plot. The bandwidth of the antenna is said to be those range of frequencies over which the return loss is greater than 7.3 dB, which is equivalent to 2.5:1 VSWR. The bandwidth of the antenna for this feed point location using IE3D at fast EM optimization is seen to be 35-MHz and a center frequency of 2.3995 GHz is obtained which is very close to the desired frequency of operation. It was observed from many trials of simulations that as the feed point location is moved away from the edge of the patch, the center frequency starts to decrease. This may be due to the highly sensitive nature of the input impedance bandwidth to position of the probe. Figure 4.3(a), 4.3(b), 4.3(c) is respectively the theoretical result, Powel optimization and the Fast EM optimization below shows the return loss snap taken during simulation. The return loss (in dB) is plotted as a function frequency.

Theoretical result (IE3D):

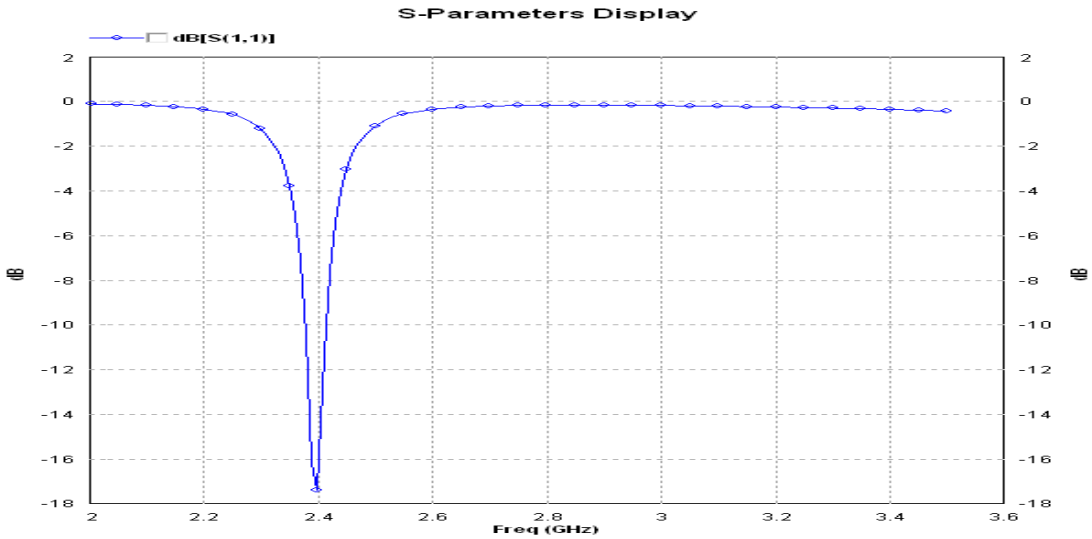

Figure 4.5(a) Return loss is -17.3309 (2.3995 GHz)

Powel Optimizer (IE3D) result:

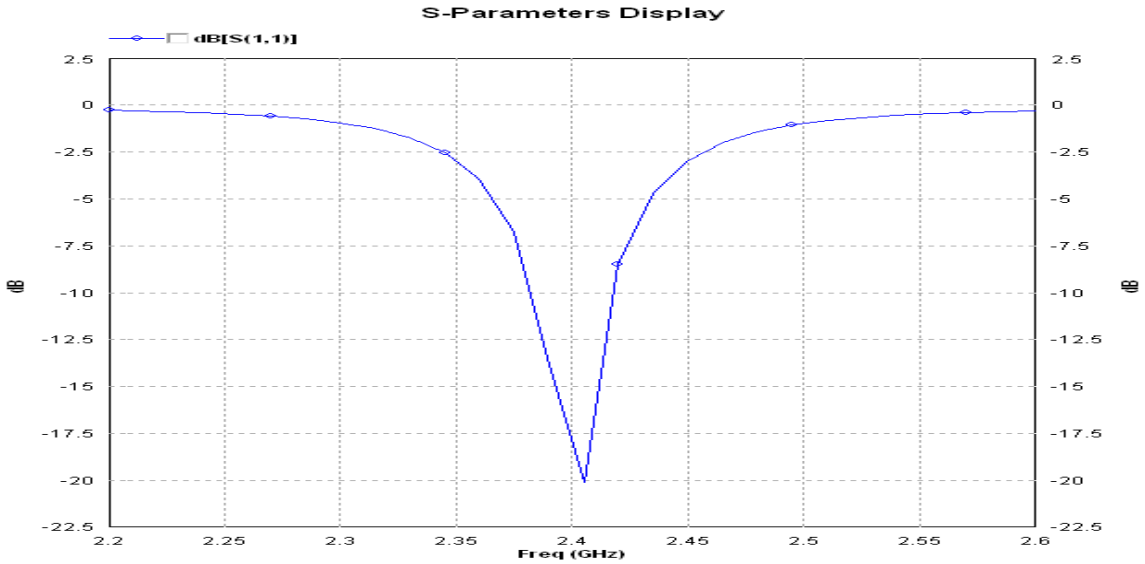

Figure 4.5(b) Return loss is -19.4796 (2.40582 GHz)

Fast EM Optimization:

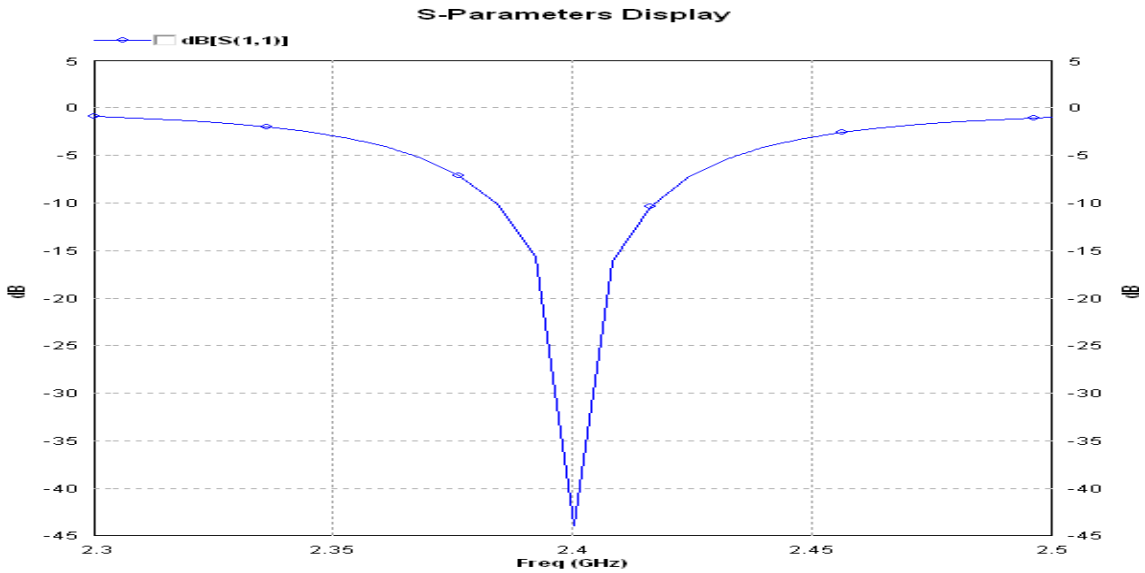

Figure 4.5(c) Return loss is -43.8848 (2.40002 GHz)

4.4.3 Input Impedance

As has been stated in Chapter 2, we expect pure real impedance at frequencies where the patch resonates, that is, where the patch is designed to radiate. As a result, the input impedance plot in Fig 4.4(a), 4.4(b), 4.4(c) respectively shows the theoretical result, Powel optimization and the Fast EM optimization, around the desired radiating frequency, sufficient reactance cancellation can only occur inside a narrow bandwidth. In addition, one needs to match the resonant resistance with the characteristic impedance of the feed line. A small antenna can be tuned to resonate with an appropriate addition of reactance, or it can be made to self-resonate so that the reactance cancellation at resonance happens naturally in the antenna structure. Since adding external reactance for this purpose increases the power loss and it also requires extra space, it is advisable to follow the second alternative

Theoretical result (IE3D):

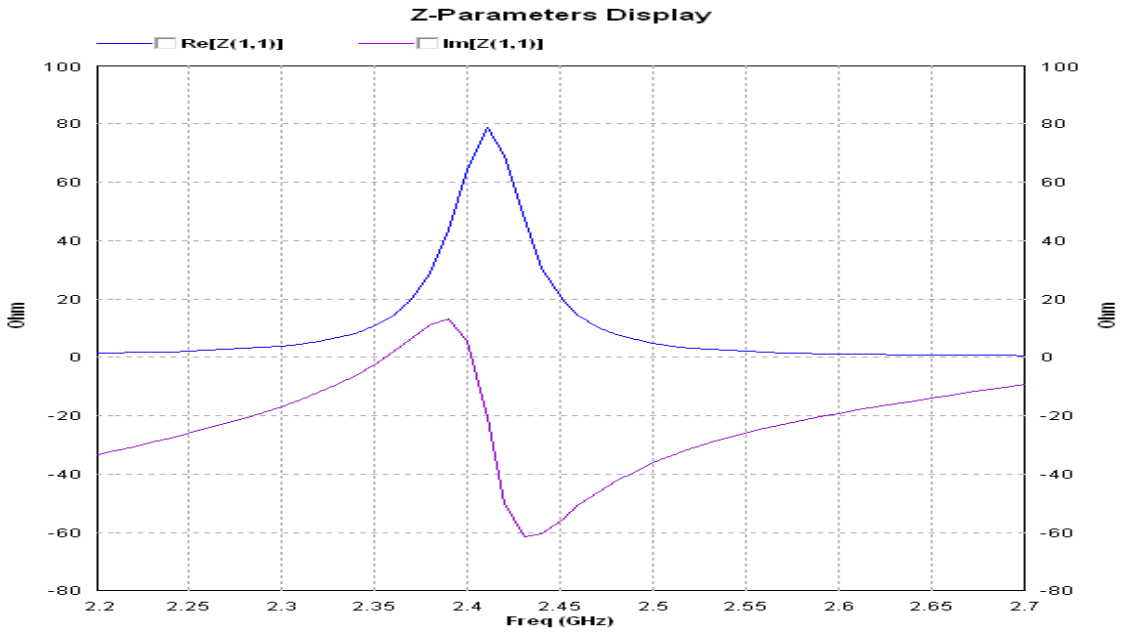

Figure 4.6(a) Input Impedance at 2.3995GHz is 60 Ω

Powel Optimizer (IE3D) result:

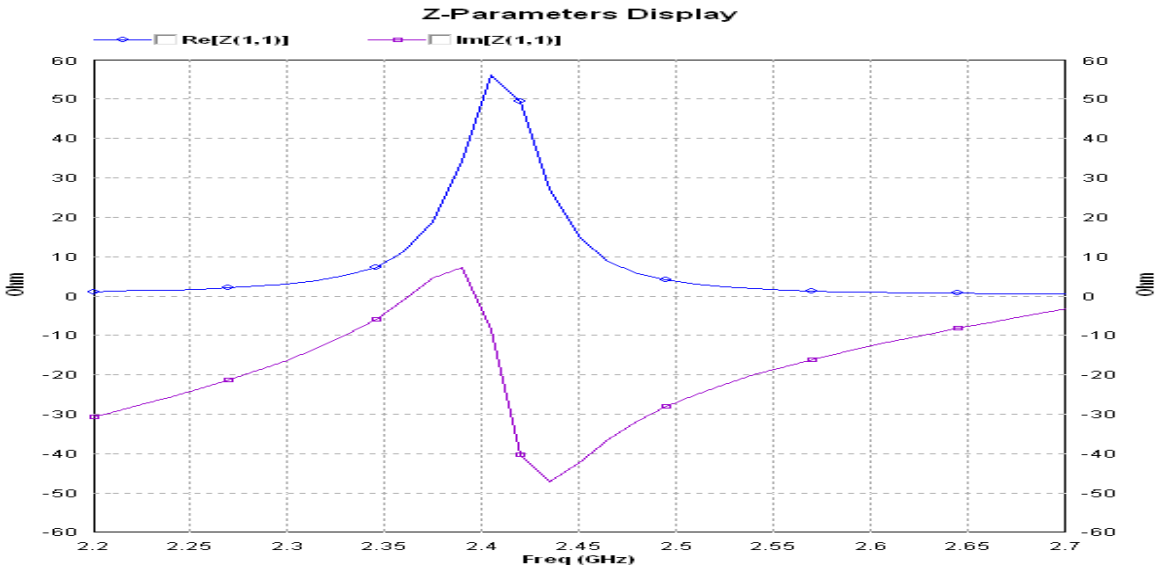

Figure 4.6(b) Input Impedance at 2.40582GHz is 50 Ω

Fast EM Optimization:

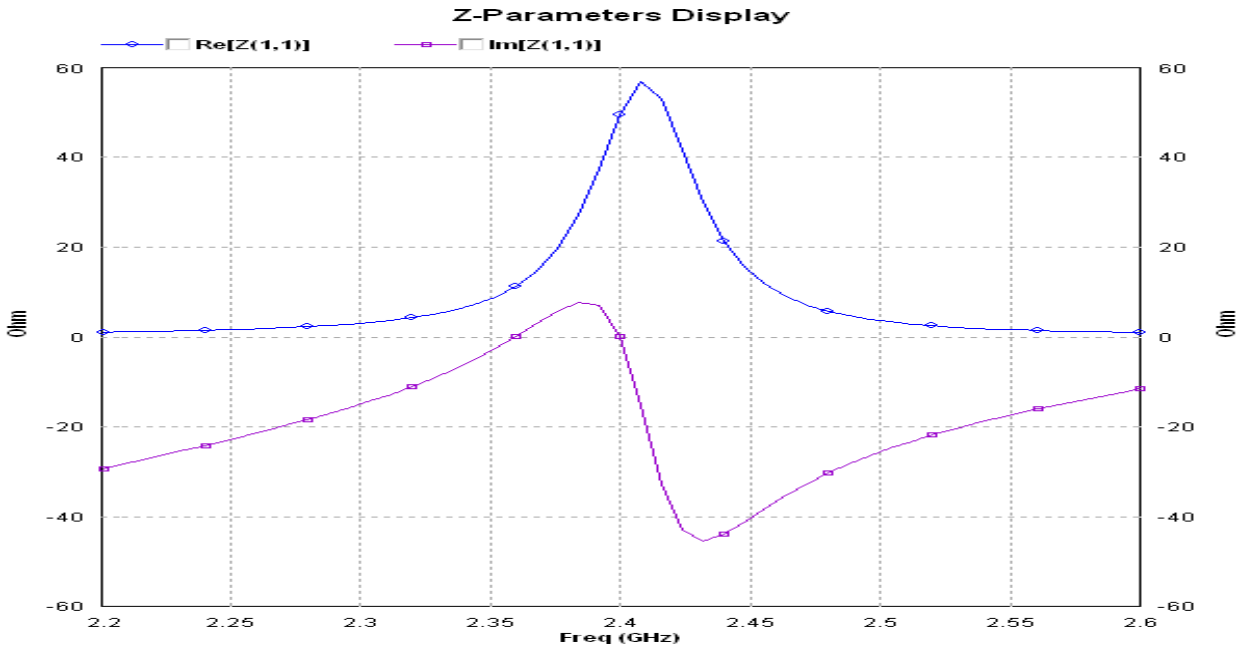

Figure 4.6(c) Input Impedance at 2.40002GHz is 50 Ω

4.4.4 Radiation Pattern Plot

A Microstrip patch antenna radiates normal to its patch surface. The elevation pattern for Φ=0 and Φ=90 degrees would be important. Figure4.5 (a), 4.5(b) and 4.5(c) below show the 2D radiation pattern of the antenna at the designed frequency for Φ=0 and Φ=90 degrees.

Theoretical result (IE3D):

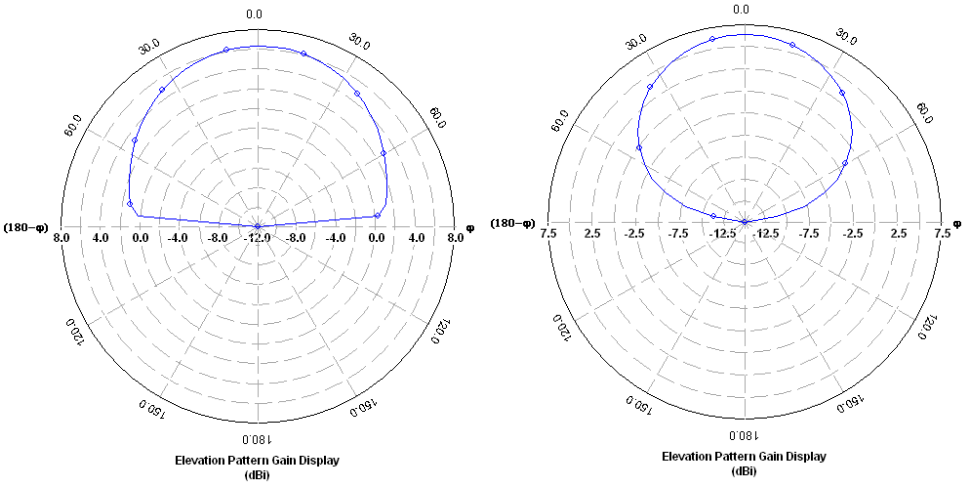

Figure 4.7(a) Elevation Pattern for Φ=0 and Φ= 90 degrees at f=2.3995 GHz

Powel Optimizer (IE3D) result:

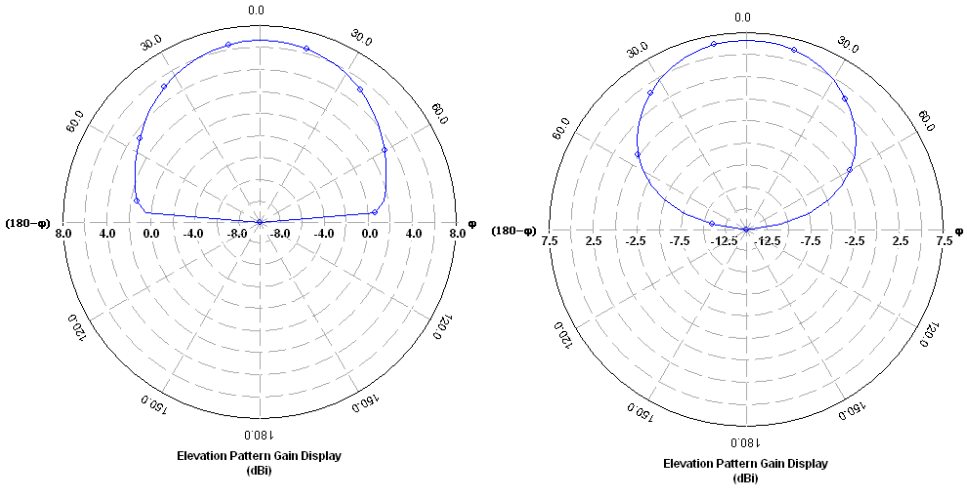

Figure 4.7(b) Elevation Pattern for Φ=0 and Φ= 90 degrees at f=2.40582GHz

Fast EM Optimization:

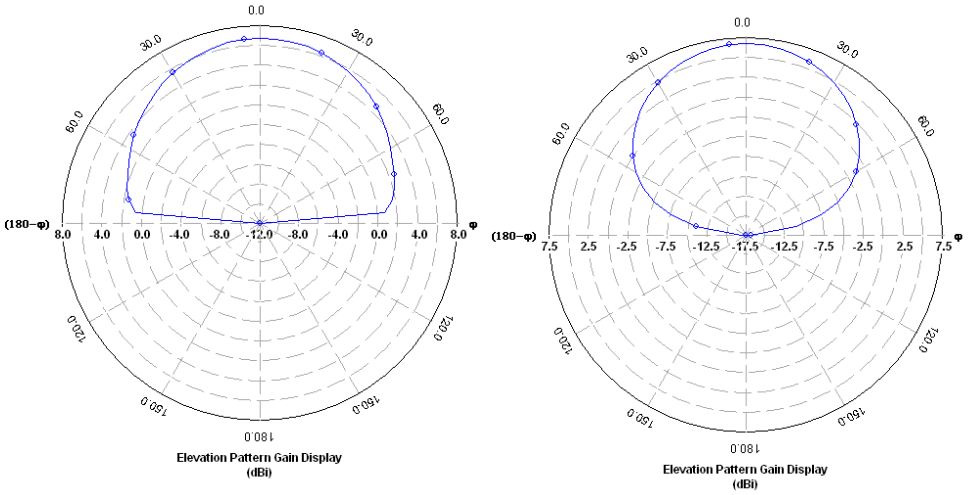

Figure 4.7(c) Elevation Pattern for Φ=0 and Φ= 90 degrees at f=2.40002 GHz

In conclusion, it can be seen from the simulation results that, the antenna performs well at the operating frequency. There is also some deviation from the theoretically expected operating frequency, the main reason for this is the discretization applied during simulation. Also from the radiation pattern seen above, maximum of the energy radiated is away from the user's head, which guarantees that an acceptable level for the specific absorption rate by the user's head can be maintained. But as can be seen from the return loss snap taken from the simulation, one can see that the whole of the 2.4 GHz band is not covered by the antenna bandwidth, therefore some work is needed to be done to tackle this.

4.4.5 Gain vs. Frequency Plot

In Microstrip patch antenna the gain is between 5-8 dB. The figure 4.8(a), 4.8(b), and 4.8(c) respectively shows the theoretical result, Powel optimization and the Fast EM optimization at the desired frequency. In frequency 2.4 GHz the gain is maximum when using the Fast EM Optimization technique.

Theoretical result (IE3D):

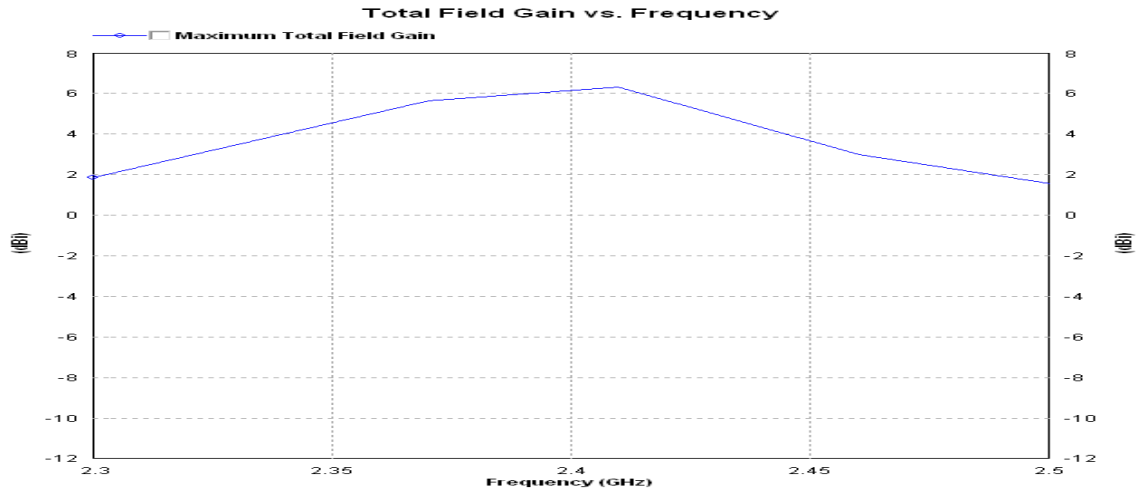

Figure 4.8(a) Gain of the patch is 6 dB at f=2.3995 GHz

Powel Optimizer (IE3D) result:-

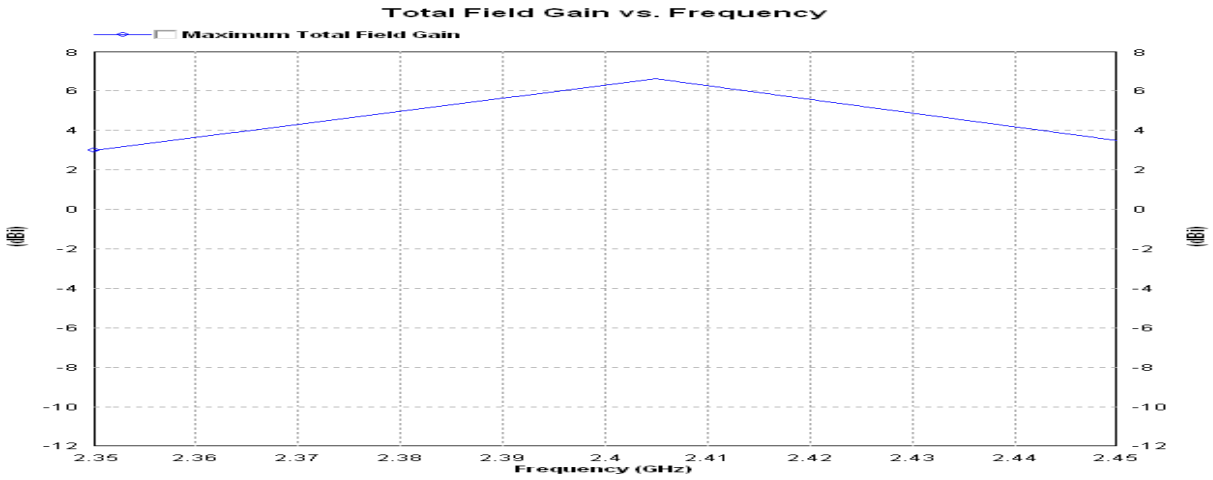

Figure 4.8(b) Gain of the patch is 6.61 dB at f=2.40582 GHz

Fast EM Optimization:

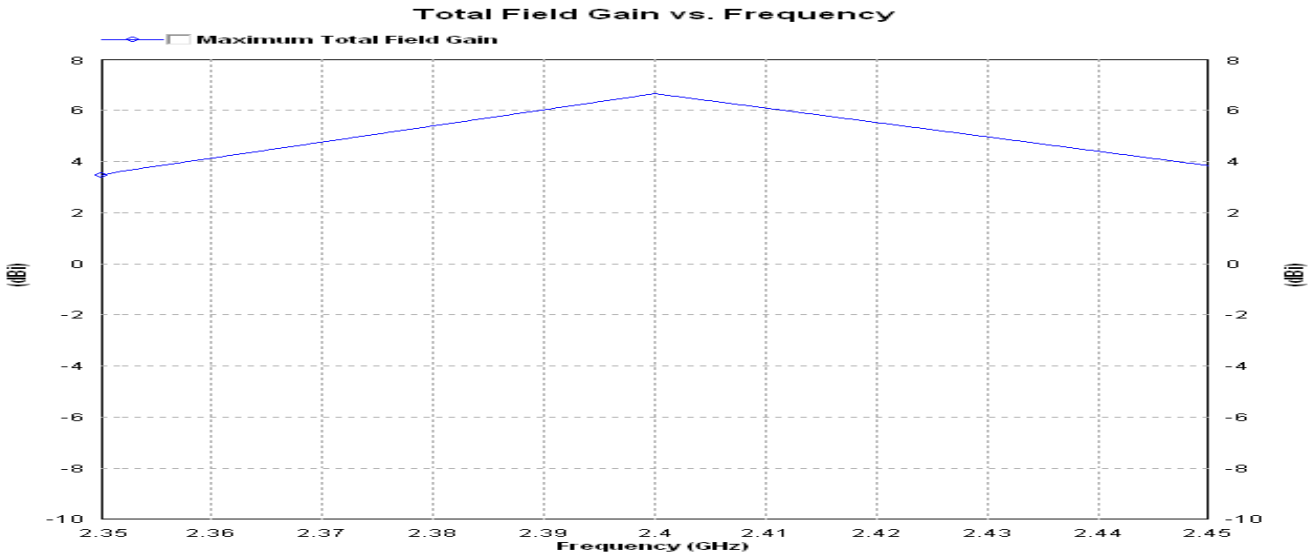

Figure 4.8(c): Gain of the patch is 6.61 dB at f= 2.40002 GHz

4.4.6 VSWR Plot

Voltage standing wave ratio (VSWR) of Microstrip antenna shown in figure 4.9(a), 4.9(b), 4.9(c) respectively shows the theoretical result, powel optimization and the Fast EM optimization of the patch. In case of Microstrip patch antenna the value of VSWR is always less than 2. At f= 2.4 GHz the value of VSWR is 1.01 using the Fast EM Optimization.

Theoretical result (IE3D):

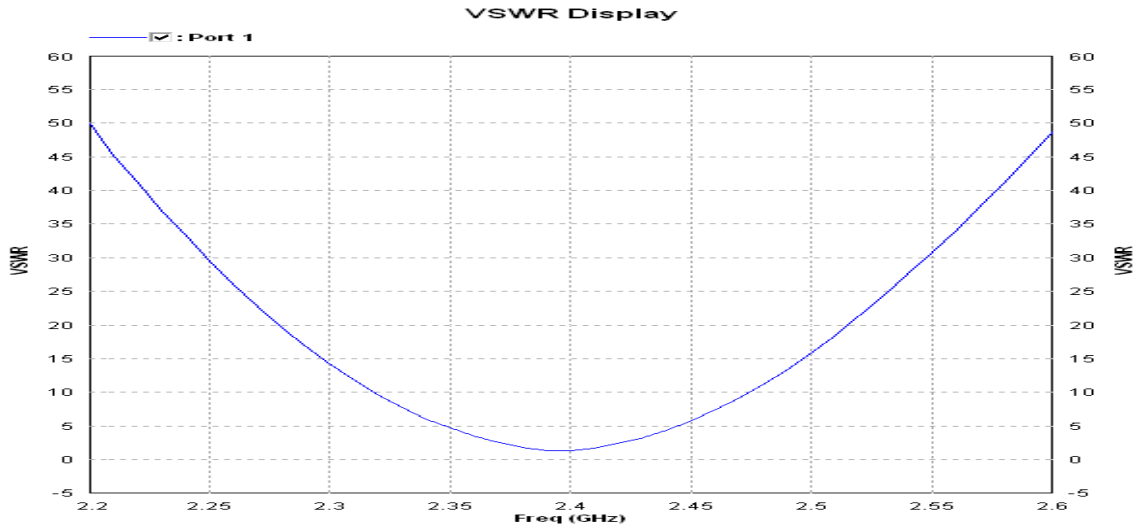

Figure 4.9(a) VSWR of Microstrip patch antenna is 1.31 at f=2.3995

Powel Optimizer (IE3D) result:

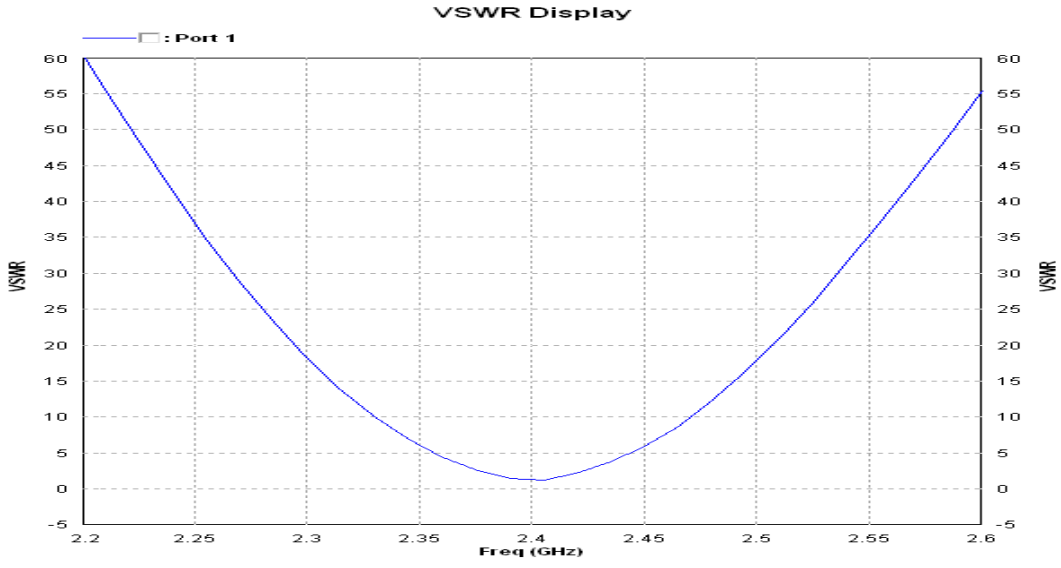

Figure 4.9(b) VSWR of Microstrip patch antenna is 1.25 at f=2.405 GHz

Fast EM Optimization:

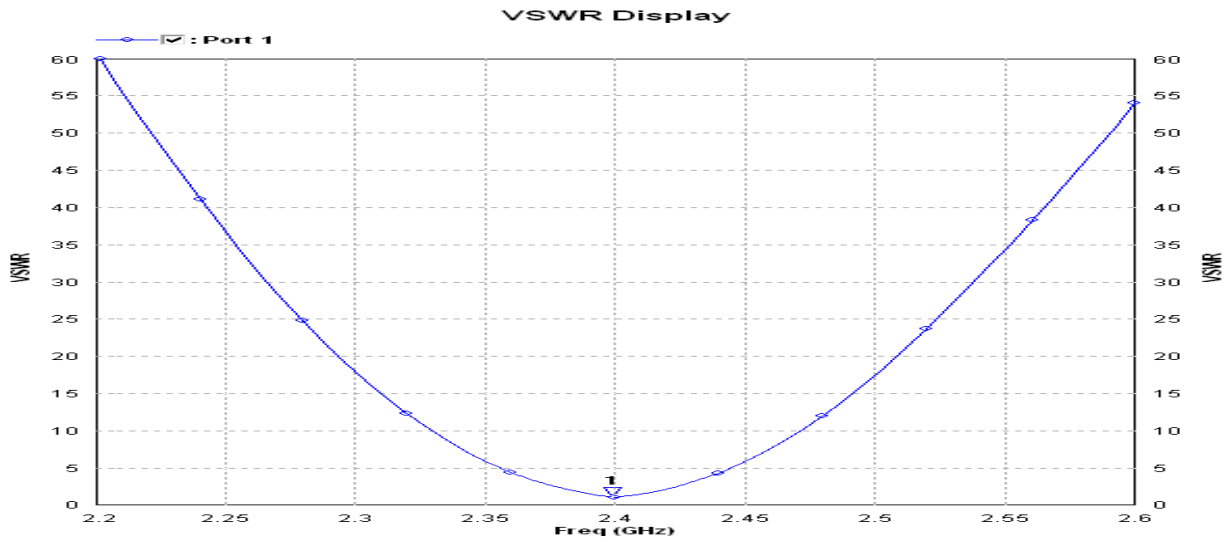

Figure 4.9(c): VSWR of Microstrip patch antenna is 1.01 at f=2.40002GHz

4.5 Compression between the Theoretical, Powel Optimization and Fast EM Optimization results

Antenna Parameter	Theoretical(IE3D)	Powel optimizer (IE3D)	Fast EM Optimization
Length(L)	47.9	47.9	49
Width(W)	39.6	39.483	39.6226
Inset Depth(y_0)	13	12.75	13.2698
Return loss (dB)	-17.3309	-19.4796	-43.8848
Impedance(Ω)	60	50	50
VSWR	1.31	1.25	1.01

Table 4.2 Compression between the Theoretical, Powel Optimization and Fast EM Optimization results

CHAPTER 5

DUAL BAND MICROSTRIP ANTENNA

5.1 Dual-Band Antenna Concept

In principle, multi-band planar antennas should operate with similar features, both in terms of radiation and impedance matching, at two or more separate frequencies. It is known, a simple rectangular Microstrip patch can be regarded as a cavity with magnetic walls on the radiating edges. The first three modes with the same polarization can be indicated by TM_{10}, TM_{20} and TM_{30}. TM_{10} is the mode typically used in practical applications; $TM_{20}$and TM_{30} are associated with a frequency approximately twice and triple of that of the mode. This provides the possibility to operate at multiple frequencies. In practice, the TM_{20} and the TM_{30} modes cannot be used owing to the facts that the TM_{20} pattern has a broadside null and the pattern has grating lobes.

The simplest way to operate at dual frequencies is to use the first resonance of the two orthogonal dimensions of the rectangular patch, i.e., the TM_{10} and the TM_{01} modes. In this case, the frequency ratio is approximately equal to the ratio between the two orthogonal sides of the patch. The obvious limitation of this approach is that the two different frequencies excite two orthogonal polarizations. Anyway, this simple method is very useful in low-cost short-range applications, where polarization requirements are not pressing.

The most popular technique for obtaining a dual-frequency behavior is to introduce a reactive loading to a single patch, including stubs[3], notches [7], pins [5] and [8], capacitors [6], and slots [9-12]. In [6-10], by these reactive-loading approaches, one can modify the resonant mode of the patch, so that the radiation pattern of the higher order mode could be similar to that of the fundamental mode. This indicates that the use of a single feed for both frequencies on a single radiating element can be realized. In 1995, a rectangular patch with two narrow slots etched close to and parallel to the radiating edge was used to obtain the dual-frequency operation

proposed by S. Maci [7]. In this dual-frequency design, the two operating frequencies are associated with the TM_{01} and TM_{30} modes of the unslotted rectangular patch. In addition, this two operating frequencies have the same polarization planes and broadside radiation patterns, with a frequency ratio within the range of 1.6-2.0 for the inset feed case

The above approach characterizes a first category of dual-frequency patch antennas, which will be identified as 1) orthogonal mode dual-frequency patch antenna [9] . This category can be extended to any kind of patch shape that offers two cross-polarized resonant modes. Most of the other dual-frequency patch antennas found in the literature can be subdivided into 2) multi-patch dual frequency antennas [9], and 3) reactively-loaded dual-frequency patch antennas [9].

5.2 Geometry of Proposed Dual Band Antenna

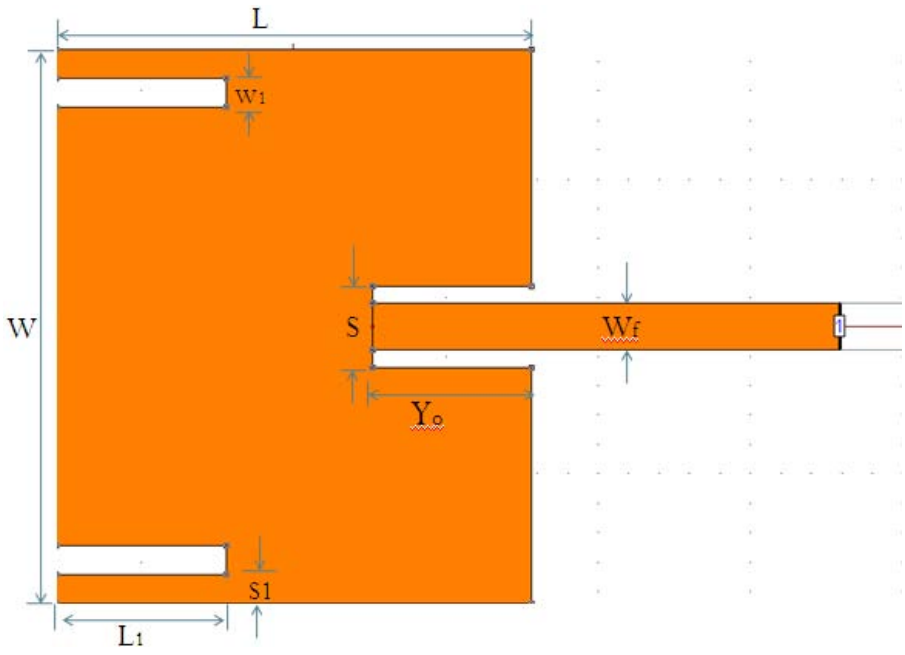

Figure 5.1 Geometry of dual band antenna

Calculation of length (L) and width (W) of Microstrip patch antenna is discussed in chapter 4 when we creating a single band Microstrip antenna. In Table 5.1 shows the parameter of Dual-Band Rectangular Microstrip antenna.

Design of Dual Band Microstrip Patch Antenna	
Width of the Patch(W)	46.9 mm
Effective dielectric constant of the Patch,(ε_{eff})	2.2922
Length of the Patch(L)	39.6 mm
Input Resistance of the Patch(R_{in})	50 Ω
Inset Depth of the Patch(y_0)	13 mm
Width of Microstrip line (w_f)	4.2 mm
Width of slots(w_1)	1.4 mm
Length of slots(L_1)	14.2 mm
Width of non-radiating edge(s_1)	1.4 mm

Table 5.1 Calculated result of Dual Band rectangular patch antenna

5.3 Dual Band Antenna Design Method

The antenna structure (Fig. 5.1) consists of a rectangular patch with two slots into one of the radiating edges, and is excited using an inset planar feed. The patch design consists of two stages. The first stage involves the creation of an additional $TM_{0\delta}$ resonant mode at a with a resonant frequency above that of the fundamental TM_{01} mode, with the same polarization sense.

The second stage is to simultaneously reduce the input impedance of both modes to 50Ω at resonance through the use of an inset feed.

Stage 1: Creation of Two Resonant Modes

The first point to note in the design process is the effect of slot separation on the patch design. With reference to the value of slot separation, experimental results have shown that placing the slots close to the nonradiating edges of the patch increases the effect of slot length on resonant frequency. This gives greater freedom to tune the resonant frequency of the $TM_{0\delta}$ mode. In view of this design, $\boldsymbol{s_1}$ has been fixed at 1.4 mm. considering the value of slot width $\mathbf{w_1}$, the requirement to achieve impedance matching of both TM_{01} and $TM_{0\delta}$ modes effectively place a constraint on this value. Increasing the slot width produces an increase in input impedance of the TM_{01} mode. As the slot width increases further, a stage is reached where the input impedance is too high for traditional impedance matching. A further reason for placing a limit on the value of slot width is the fact that the resonant frequency of the TM_{01} mode remains largely unaffected. For this design, experimental results indicate that the slot-width value should not exceed 3 mm. Placing this constraint on the slot-width value is beneficial from a designer's point of view, as only the effect of slots on the additional mode need be considered. This reduces the complexity of the design process. Regarding the effect of slot length L_1 on creating an additional $TM_{0\delta}$ mode, experimental results indicate that the slot length *l*1 must take on a value of between 40% L and 56% L. Increasing L_1 within these constraints can produce a frequency ratio of between 1.03 and 1.29.

Stage 2: Achieving Impedance Matching at Both Frequencies

The first part of the impedance-matching procedure is to produce an equal value of input impedance at both resonant frequencies. This has been achieved by varying the slot width

w_1.when we increase $\mathbf{w_1}$ the value of input impedance changes. The final stage in the design process involves the use of an inset feed. It is found that increasing the inset feed length $y_0$can simultaneously reduce the input impedance at both frequencies to **50Ω**. The inset feed has a slight effect on both resonant frequencies and thus slight tuning is required.

5.4 Results and Discussion

5.4.1 Return loss and Antenna Bandwidth

The Inset feed and the two slots used to design the dual band rectangular Microstrip patch antenna. The center frequency is selected as the one at which the return loss is minimum. As described in chapter 2, the bandwidth can be calculated from the return loss (RL) plot. The bandwidth of the antenna for this dual frequency point location using IE3D at fast EM optimization is seen to be$f_1 = 2.4\,GHz$ and due to slots the second frequency is $f_2 = 3.08\,GHz.$ .The frequency ratio is 1.29 for using these dual slots. Figure 5.2(a), 5.2(b), 5.2(c) respectively the theoretical results, Powel optimization and the Fast EM optimization are shown below. The return loss (in dB) is plotted as a function frequency.

Theoretical result (IE3D):

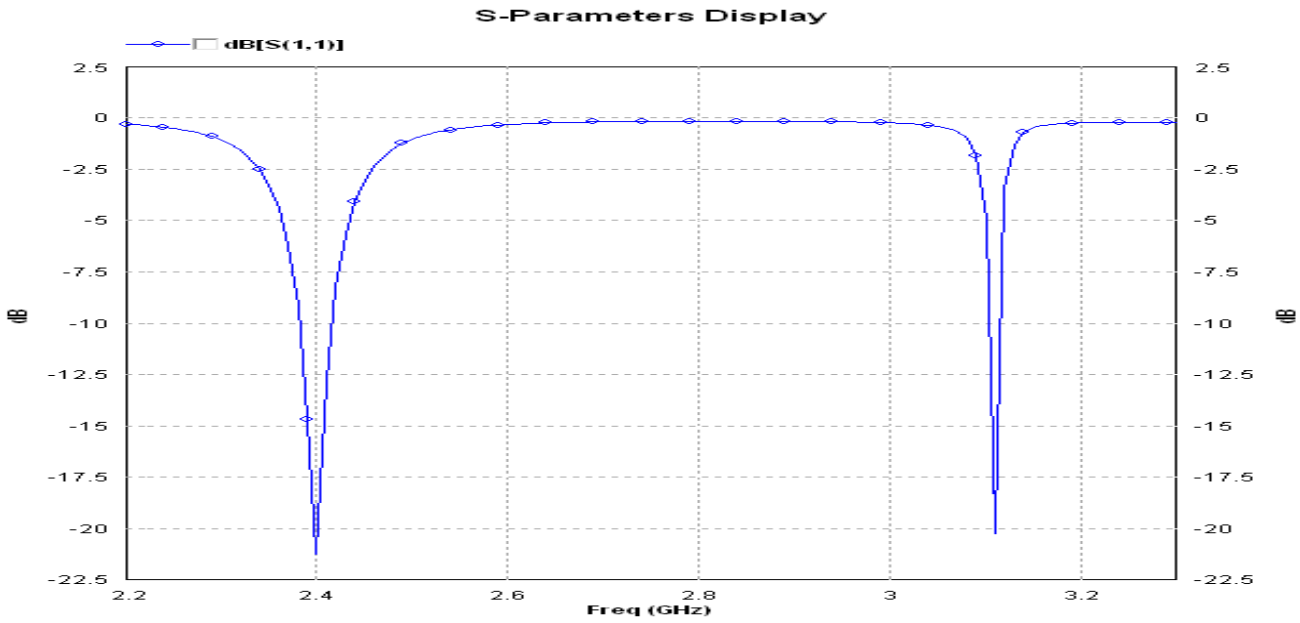

Figure 5.2(a) Return loss is -21.124dB (2.3998 GHz) and Return loss is -20.1766dB (3.1103 GHz)

Powel Optimizer (IE3D) result:

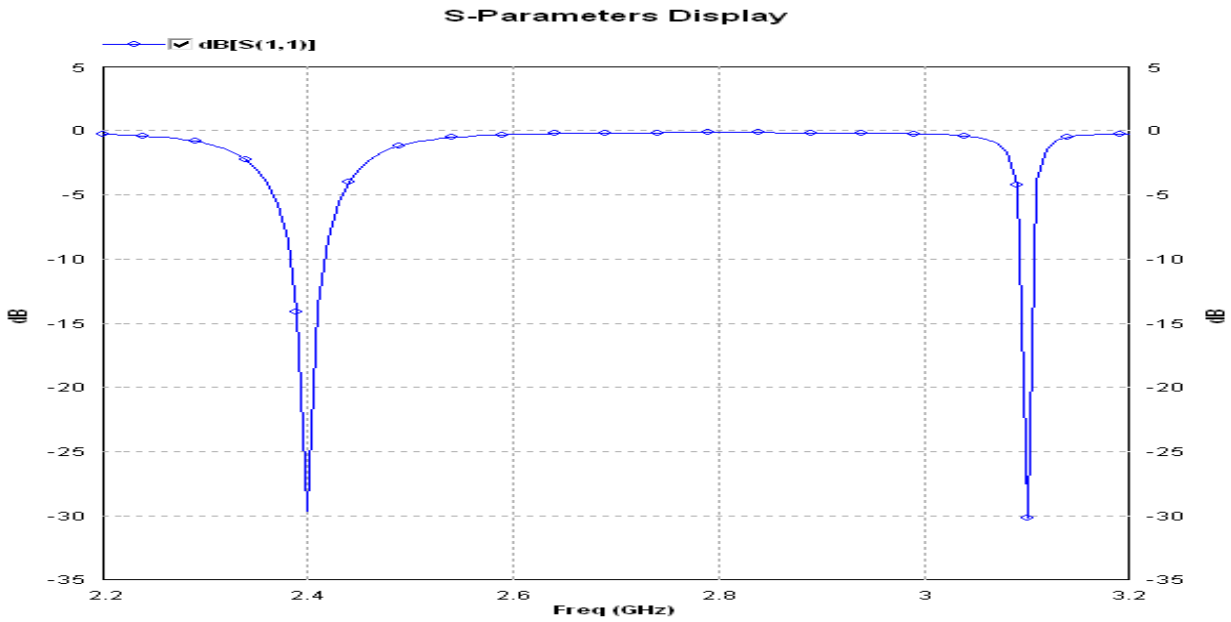

Figure 5.2(b) Return loss is -29.6008 (2.3995 GHz) and Return loss is –30.057 (3.1004 GHz)

Fast EM Optimization:

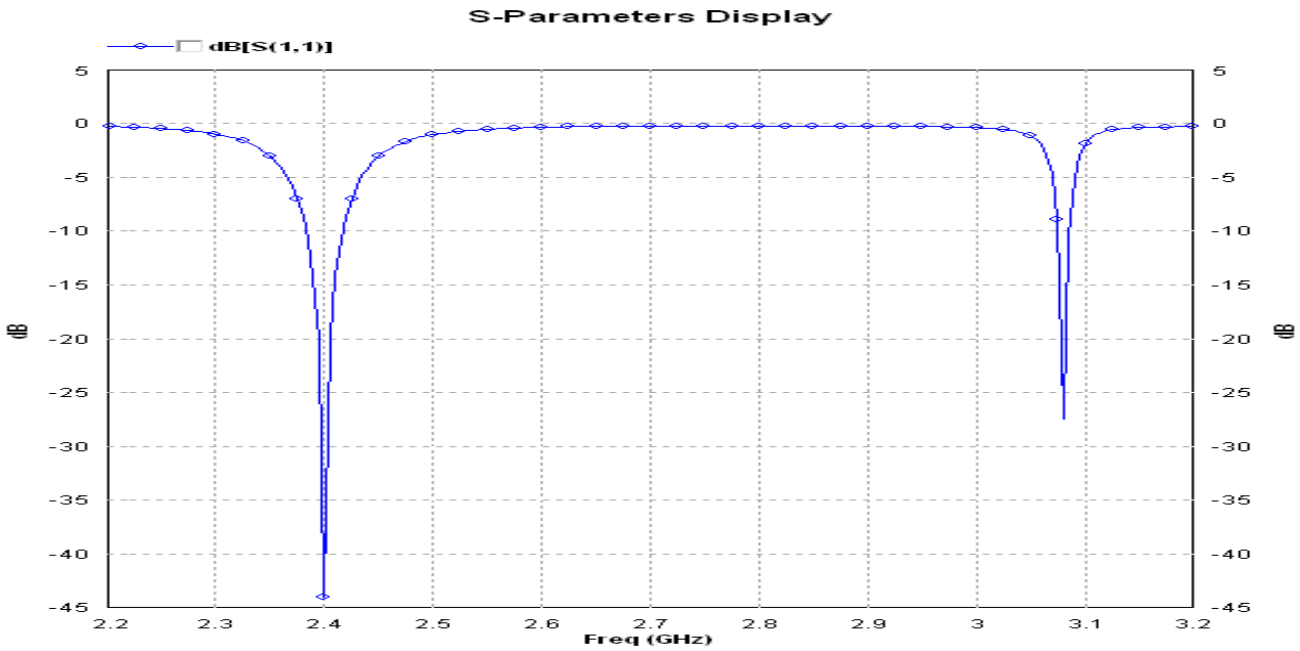

Figure 5.2(c) Return loss is -43.95 (2.4 GHz) and return loss is -27.4144 (3.08 GHz)

Radiation pattern plot

A Microstrip patch antenna radiates normal to its patch surface. The elevation pattern for Φ=0 and Φ=90 degrees would be important. Figure5.3(a), 5.3(b) and 5.3(c) below show the 2D radiation pattern of the antenna at the designed frequency for Φ=0 and Φ=90 degrees

Theoretical result (IE3D):

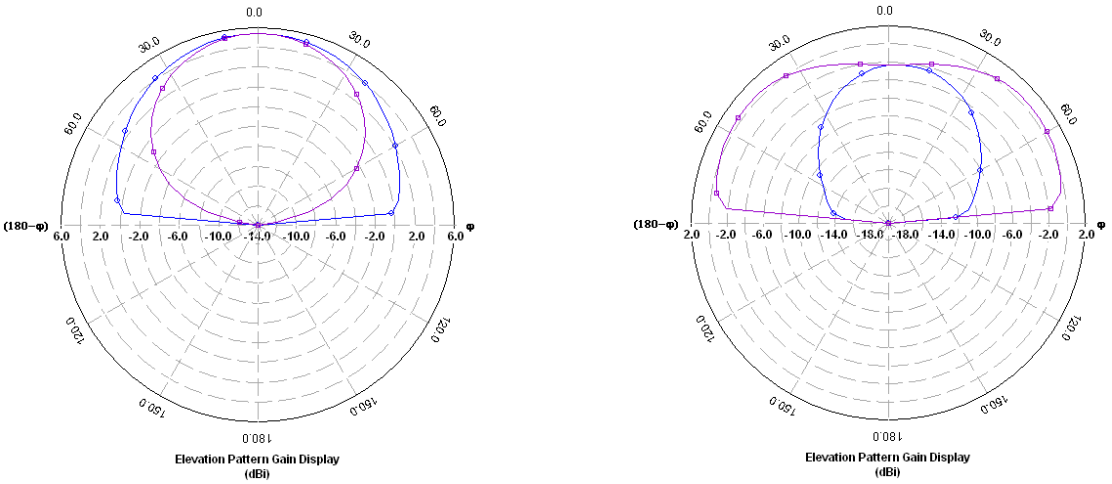

(i) *(ii)*

Figure 5.3(a) (i) Elevation Pattern for Φ=0 and Φ= 90 degrees at f=2.3998 GHz
(ii) Elevation Pattern for Φ=0 and Φ= 90 degrees at f=3.1 GHz

Powel Optimizer (IE3D) result:

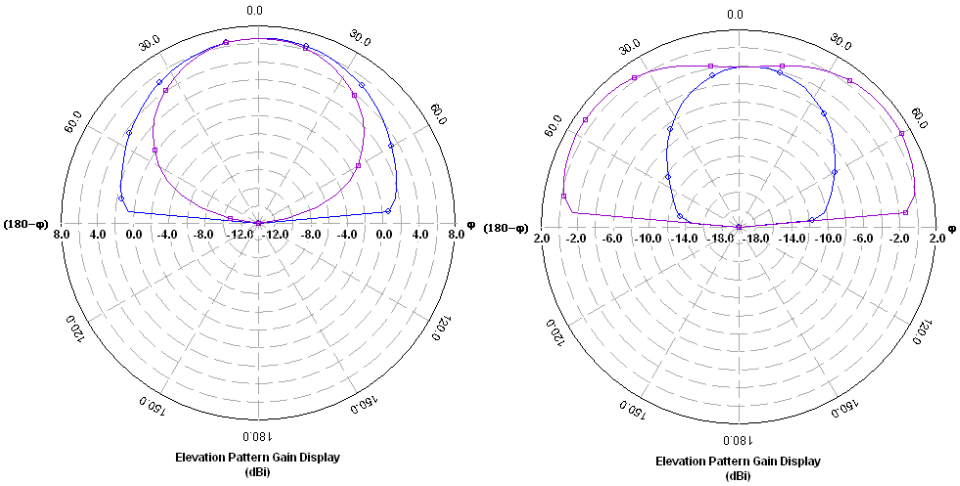

Figure 5.3(b) (i) Elevation Pattern for Φ=0 and Φ= 90 degrees at f=2.3995 GHz
(ii) Elevation Pattern for Φ=0 and Φ= 90 degrees at f=3.1004 GHz

Fast EM Optimization:

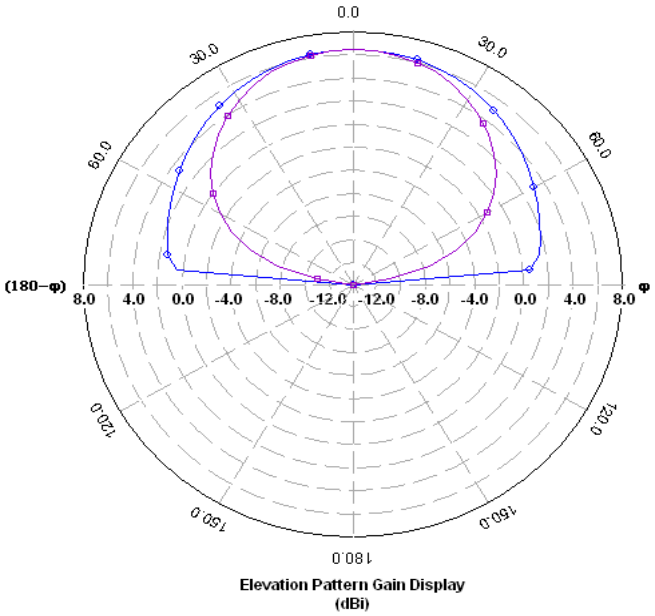

(i)

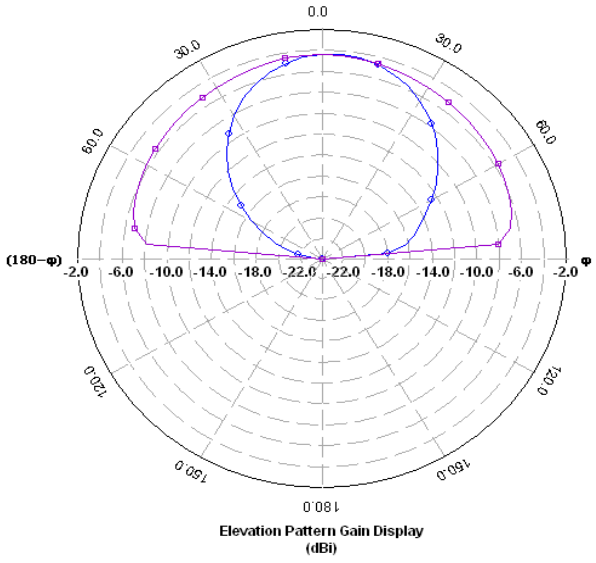

(ii)

Figure 5.3(c) (i) Elevation Pattern for Φ=0 and Φ= 90 degrees at f=2.4 GHz
(ii)Elevation Pattern for Φ=0 and Φ= 90 degrees at f=3.08 GHz

VSWR Plot

Voltage standing wave ratio (VSWR) of Microstrip antenna shown in figure 4.7(a), 4.7(b), 4.7(c) respectively shows the theoretical result, Powel optimization and the Fast EM optimization of the patch. In the case of Microstrip patch antenna the value of VSWR is always less than 2 . At f_1= 2.4 GHz the value of VSWR is 1.08 and at $f_2 = 3.08\ GHz$ the value of VSWR is 1.3 using the Fast EM Optimization.

Theoretical result (IE3D):

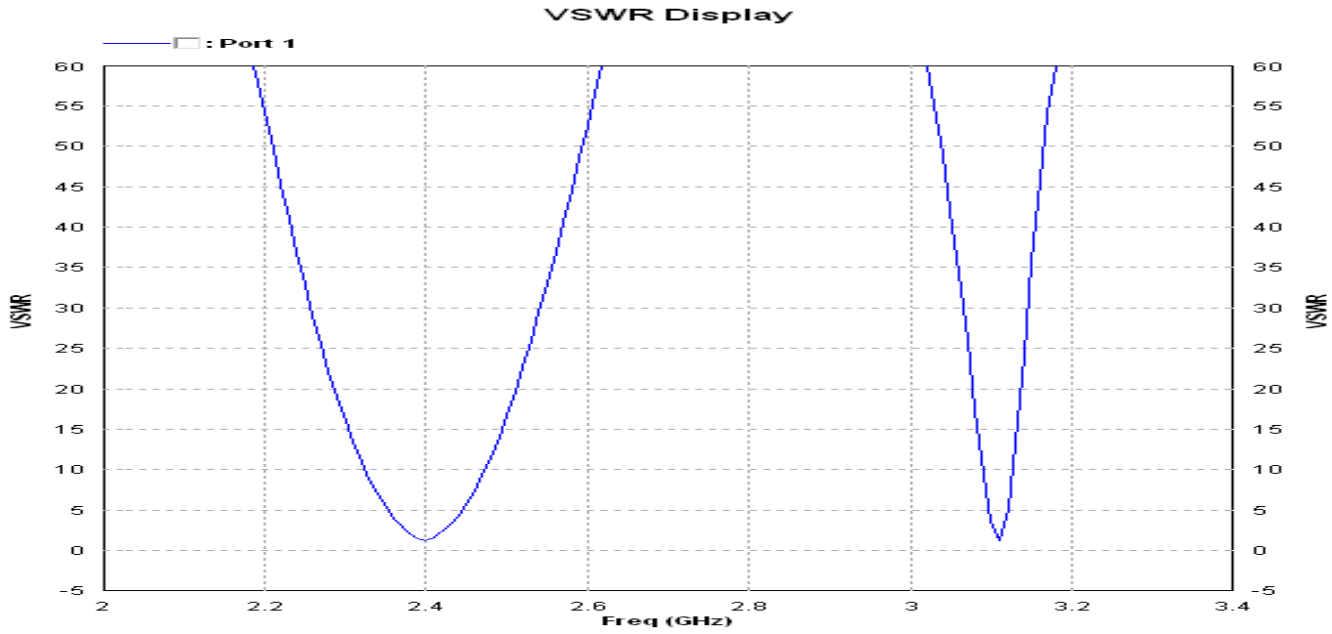

Figure 5.4 (a) VSWR of Microstrip patch antenna is 1.27 at f_1=2.3995 GHz and 1.37 at f_1=3.1103GHz

Powel Optimizer (IE3D) result:

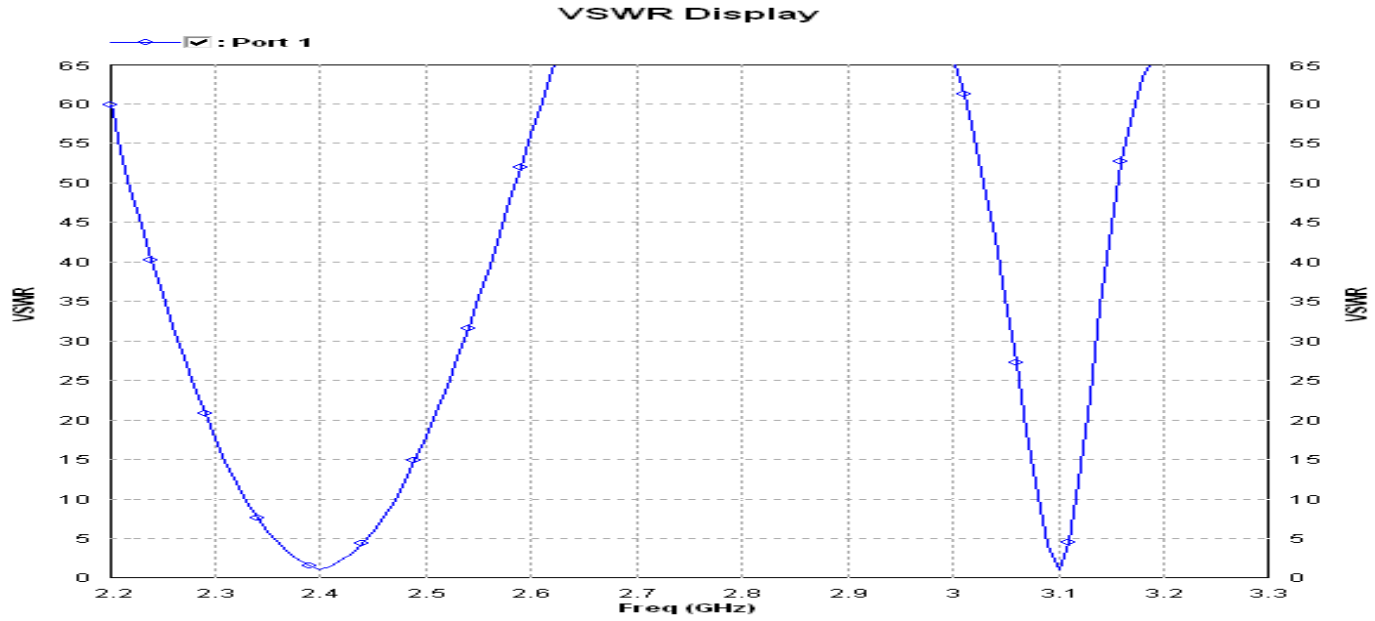

Figure 5.4(b) VSWR of Microstrip patch antenna is 1.15 at f_1=2.3995 GHz and 1.12at f_1=3.1004 GHz

Fast EM Optimization:

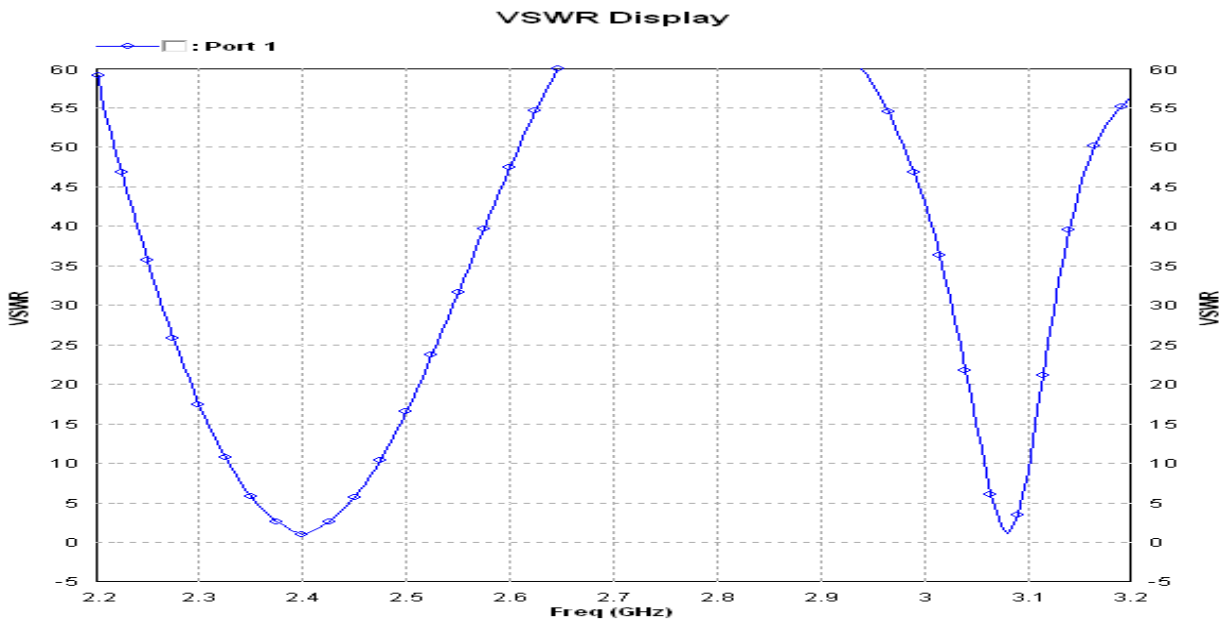

Figure 5.4(c) VSWR of Microstrip patch antenna is 1.27 at f_1=2.4 GHz and 1.37 at f_1=3.08GHz

5.5 Compression between the Theoretical, Powel Optimization and Fast EM Optimization results of dual band antenna.

Antenna Parameter	Theoretical (IE3D)		Powel optimizer (IE3D)		Fast EM Optimization	
Length(L)[mm]	47.9		47.9		49	
Width(W)[mm]	39.6		39.483		39.6226	
Inset Depth(y_0)[mm]	13		12.75		13.2698	
Slot Length(L_1)[mm]	14.2		14.323		14.2	
Slot Width(w_1)[mm]	1.4		1.4		1.4	
Frequency(f1)[GHz] And Return loss (dB)	2.3998(-21.1524)		2.3995(-29.6008)		2.4(-43.9544)	
Frequency(f1)[GHz] And Return loss (dB)	3.1103(-20.1766)		3.1004(-30.137)		3.08002(-27.4144)	
Impedance(Ω)	60		50		50	
VSWR	$f_{1(2.3998)}$	$f_{2(3.1103)}$	$f_{1(2.3995)}$	$f_{2(3.1004)}$	$f_{1(2.4)}$	$f_{2(3.08002)}$
	1.27	1.37	1.15	1.12	1.08	1.3

Table 5.2 Compression between the Theoretical, Powel Optimization and Fast EM Optimization results of dual band antenna

CHAPTER 6

PARTICLE SWARM OPTIMIZATION

6.1 Background

When dealing with optimization of engineering problems, the functions considered are often very complex, multi-dimensional and might be both continuous and discrete within the solution domain. Since calculus no longer applies, analytic evaluation can no longer be used to find points of minimum or maximum. Intuitively, the need for a smart scheme that makes guesses based on the relative solution fitness is evident.

In 1995 James Kennedy and Russell Eberhart presented particle-swarm optimization (PSO), an optimizer that models the behavior and intelligence of a swarm of bees, school of fish or flock of birds, and emphasizes both social interaction and nostalgia from the individual's perspective.

Kennedy and Eberhart formed a research duo of a social psychologist and an electrical engineer, whose work has had a great impact on the electromagnetic community. PSO is intuitive, easy to implement and has been proven to outperform other and more intricate methods like genetic algorithms.

6.2 Genetic algorithms

A basic understanding of genetic algorithms (GAs) is preferable when dealing with other optimization techniques, thus a short introduction will be given in this section. GAs were introduced in the early 70s by John Holland, and is sprung from evolutionary computing, invented in the 60s.

Gases rely on the principals of Darwin's theory of evolution. In optimization applications the concept of survival of the fittest combined with selection and adaptation, provides robust and stochastic search methods. Being effective in optimizing complex, multidimensional functions in a near-optimal fashion, GAs have proven successful in a vast amount of engineering problems.

Since GAs model evolution they, in essence, share paradigm with genetics. The key concepts are [14];

- Genes - A parameter is generally equivalent to a gene. Some sort of coding or mapping translates a parameter value into a gene,
- Chromosomes - A string of genes is referred to as a chromosome. In a 3D example three genes would together form a trail solution. This solution is equivalent to a chromosome or a position,
- Population - A set of solutions is called a population,
- Generation - Iterations in the GA,
- Parent - A pair of existing chromosomes are selected from the population for mating or recombination,
- Child - The offspring of the parents, and
- Fitness - There must be a way to tell how fit an individual is. Often, there exists a function which given a chromosome returns a fitness value.

The main idea is to represent parameters as genes in chromosomes. Valid chromosomes are grouped in a population, from which fit parents are selected to produce new chromosomes by recombination and mutation.

One reason for the fact that GAs are being considered complex and untidy to implement, is the many options associated with the selection, recombination and mutation [15]. The PSO, on the other hand, only concerns one major operation. This operation is the velocity calculation, which will be discussed in the following sections.

6.3 Theory

Since PSO models swarm behavior, this section takes of from a somewhat informal point of view. Imagine a swarm of bees looking for the most fertile feeding location in a field. Each bee has a location in the three-dimensional space, x_m, where the parameters x_1, x_2 and x_3 are intended to constitute a point in space. The bee evaluates every position for the absolute fitness. This fitness will, for this example, be a positive number which increases with increasing fertility. The bee remembers the spot where it encountered the best fitness and also shares this information with the other bees, so that the entire swarm will know the global best position. The bee's movement is controlled by its velocity, v_m, which is influenced by its best personally, encountered location and the global best. The bee will always try to find the way back to its personal best location, while at the same time curiously moving towards the global best. If a bee finds a location that has a fitness greater than any encountered before, the entire swarm will be informed instantly and thus move towards this location. The result will be a swarming behavior, evidently based on both nostalgia and social influence.

It should be emphasized that the algorithm is considered to be continuous, i.e. the particles parameters can take on any value in the defined interval. In the previous example this means that the bee can be in any position in the field, even in the exact same spot where other bees are. Another way of describing this is to state that collisions do not occur, which of course lacks correspondence in real life.

A function that evaluates the position in solution space is needed. Though the algorithm is generic, the fitness function is often unique to a specific problem. More formally, the algorithm is [15] given below;

- Define the solution space,
- Define a fitness function,
- Randomly initialize x_m and v_m (for particle 1 to *M*),
- Reckon P_m^{bp} and p_m^{bv} (for particle 1 to *M*),
- Reckon g^{bp}andg^{bv} , and
- Until some criteria are met do (for particle 1 to *M*):
    - Evaluate current position's fitness
        - If it is better than P_m^{bv}, exchange $P_m^{bp}$and p_m^{bv}
        - If it is better than g^{bv}, exchange g^{bp} and g^{bv}
    - Reckon v_m
    - Let $x_m = x_m + v_m$ (Determine next position),

where P_m^{bp} is a vector pointing to the personal best position, and p_m^{bv} is the value associated with that position. g^{bp} and g^{bv} are in the same manner associated with the global best position. Note that the personal position and value are related to one of the *M* particles, and that the global best position and value are shared, thus equal to all individuals. The dimension is of course not limited to three, but instead *N*.

Of consistency, the reckoning of next position should read

$$x(t + \nabla t)_m = x(t)_m + v(t)_m \nabla t \qquad (3.1)$$

Though t is often omitted and Δt is implied to be 1.

PSO is considered to be unique in the sense that it explores the space wherein the solutions exist, not a space of solutions, which is a fundamental property of GAs.

6.3.1 Algorithm

The heart of the optimization is the computation of the velocity, which is analogous to the modification of the relative change, or simply change of change. The concept is to use vectors pointing from the current to the personal best and global best position, according to,

$$v(t)_{mn} = v(t-\Delta t)_{mn} + \frac{\emptyset_1\left(p_{mn}^{bp} - x_{mn}\right) + \emptyset_2\left(g_n^{bp} - x_{mn}\right)}{\Delta t}$$

Where

$$\emptyset_1 = c_1 rand()$$

And

$$\emptyset_2 = c_2 rand()$$

The constants c_1 and c_2 affect the influence of nostalgia and social interaction, respectively, whereas *rand()* is a function returning a random number from a uniform distribution in the interval [0,1]. The calls to the random function are considered to be separate, thus making them independent. Again, implying *t* and $\Delta t = 1$, a clearer representation of (3.2) is given by

$$v_{mn} = v_{mn} + \emptyset_1\left(p_{mn}^{bp} - x_{mn}\right) + \emptyset_2\left(g_n^{bp} - x_{mn}\right)$$

Throughout the report, the significance of Φ_1,Φ_2 and *rand()* will not change.

6.3.2 Boundary condition

Since Φ_1 and Φ_2 are stochastic, their presence models the slight unpredictable behavior, or craziness, of particles in a swarm [17].

If the variables can take on any value, an oscillating behavior of increasing amplitude is likely to occur if the velocity is not constrained. This is often referred to as explosion and is avoided by limiting $|v_m|$by the positive numberv_{max}.

The variables are often limited to some interval. This will introduce a need to handle particles trying to pass the boundary limit. Figure 3.1 shows three boundary conditions. The leftmost shows the absorbing-wall approaches, where the velocity in the direction of the boundary is zeroed. The following condition, the bouncing-wall approach, effects the particles while the rightmost, the invisible wall, simply lets the particles pass. An inherited condition is that no fitness evaluation will be performed beyond the boundaries. This usually reduces the number of computations drastically, since the algorithm itself is very simple compared to most fitness evaluations. Particles outside the boundaries are supposed to, on their own, find their way back to the defined space [15].

Inertial weight, *w*, is shown in (3.3) and was introduced for controlling the convergence of the algorithm. A large *w* encourages exploration, while a small *w* makes the particles fine-comb the area surrounding the global maximum. The inertial weight is there for often linearly decreased during an optimization, to speed up the convergence while covering a large area at the beginning.

$$v_{mn} = wv_{mn} + \emptyset_1\left(p_{mn}^{bp} - x_{mn}\right) + \emptyset_2\left(g_n^{bp} - x_{mn}\right)$$

The constriction factor, *K*, was introduced to make an analytical analysis of the PSO, though (3.4) can be considered a special case of (3.3) [15].

$$v_{mn} = K\left((v_{mn} + \varphi_1\, rand\,()\left(p_{mn}^{bp} - x_{mn}\right) + \varphi_2 rand()\left(g_n^{bp} - x_{mn}\right)\right)$$

where K is determined from

$$\varphi = \varphi_1 + \varphi_2 \;\; \varphi > 4$$

And

$$K = \frac{2}{\left|2 - \varphi - \sqrt{\varphi^2 - 4\varphi}\right|}$$

Combinations of empirical testing and mathematical analysis of various test cases, by means of parameter settings, are summarized in [15]. The suggested settings are c_1 = 1:49, c_2 = 1:49, and that w is linearly decreased from 0.9 to 0.4, or that K = 0:729, φ_1 = 2:8 and φ_2 = 1:3, depending on method of implementation.

Overall, a population size of $\leq$ 30, using the invisible-wall approach with the settings displayed, has proven to provide good results [15].

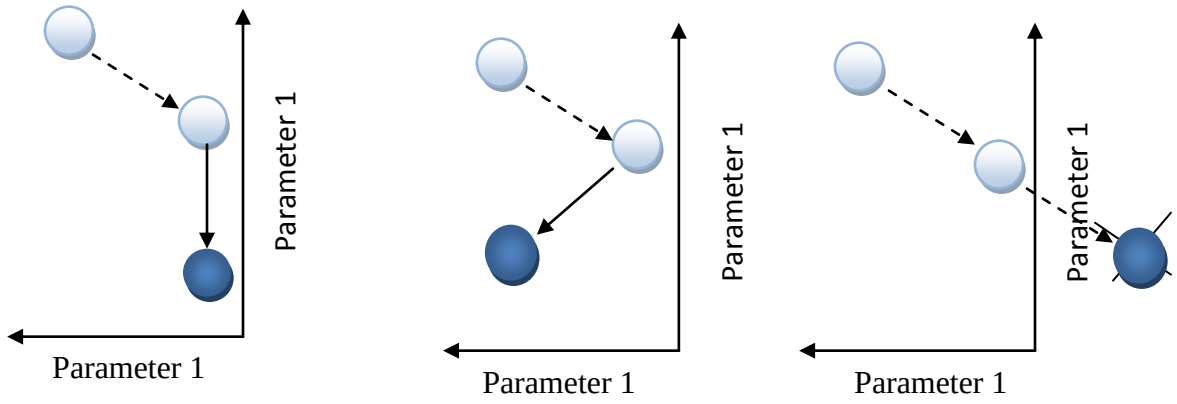

Figur6.2 Boundary condition in PSO algorithm

6.3.3 Updated Function

While the update of the velocity according to (3.10) stays the same, compared to that of the continuous version, the interpretation is now that velocity is the probability of a bit taking on a one or a zero. The meaning of the change of change is therefore evidently different. This is implemented as an IF statement,

$$\text{IF (rand() < } S(v_{mn})\text{) THEN } x_{mn} = 1 \text{ ELSE } x_{mn} = 0;$$

Where

$$S(v_{mn}) = \frac{1}{1 + e^{-v_{mn}}}$$

is called a sigmoid limiting transformation [20].

This leads to the conclusion that the probability of a bit taking on a one is $S(v_{mn})$, and $1\text{-}S(v_{mn})$ that it will be a zero. Since this holds regardless of the initial state of a bit, the probability of a bit changing must be $S(v_{mn})(1\text{- }S(v_{mn}))$. Note that this only holds if the initial state of a bit is *unknown*. This is represented in [15] as

$$p(\Delta) = S(v_{mn})(1\text{- }S(v_{mn}))$$

Thus a change in the velocity still is a change in the rate of change [20].

6.4 Comparison between GA and PSO

- **Similarity**
  - Both algorithms start with a group of a randomly generated population
  - Both have fitness values to evaluate the population.
  - Both update the population and search for the optimum with random techniques.
  - Both systems do not guarantee success.
- **Dissimilarity**
  - However, unlike GA, PSO has no evolution operators such as crossover and mutation.
  - In PSO, the potential solutions, called particles, fly through the problem space by following the current optimum particles.
  - Particles update themselves with the internal velocity.
  - They also have memory, which is important to the algorithm.

- **Advantages**
  - PSO is easy to implement and there are few parameters to adjust.
  - Compared with GA, all the particles tend to converge to the best solution quickly even in the local version in most cases

CHAPTER 7

OPTIMIZATION USING PSO

7.1 Optimization Setup of IE3D\PSO

The design and estimation of the parameters of a Microstrip patch antenna is generally complex and requires detailed mathematical approach for full-wave analysis. The antenna dimensions are critical in the quantitative estimation of the desired antenna performance with the desired accuracy in results. Many approaches [21-22] were made on the parametric study of various patch antennas. It has been found that in most patch antenna designs a trial-and-error process is almost always necessary. As for example, IE3D [9] is one of the most powerful electromagnetic simulation software for antenna design. However, the optimization software included in IE3D is insufficient for optimization of the designed parameters of an antenna [10]. Sometimes, it requires trial and error solution for getting best design values of the antenna parameters [8]. There have been several attempts for optimization of antenna design parameters using the well-known optimization techniques such as: (i) Particle Swarm Optimization (PSO) (ii) Genetic Algorithm, (iii) Simulated Annealing etc. [14] & [22]. The PSO algorithm and its variations have been found to be very suitable and relatively better method for optimization of electromagnetic problems. Thus, it is expected that a best possible optimization may be obtained by further refinement of the IE3D results with the help of PSO. Using the combination of IE3D and PSO algorithm, a design technique for patch antenna have been developed and presented in the following sections.

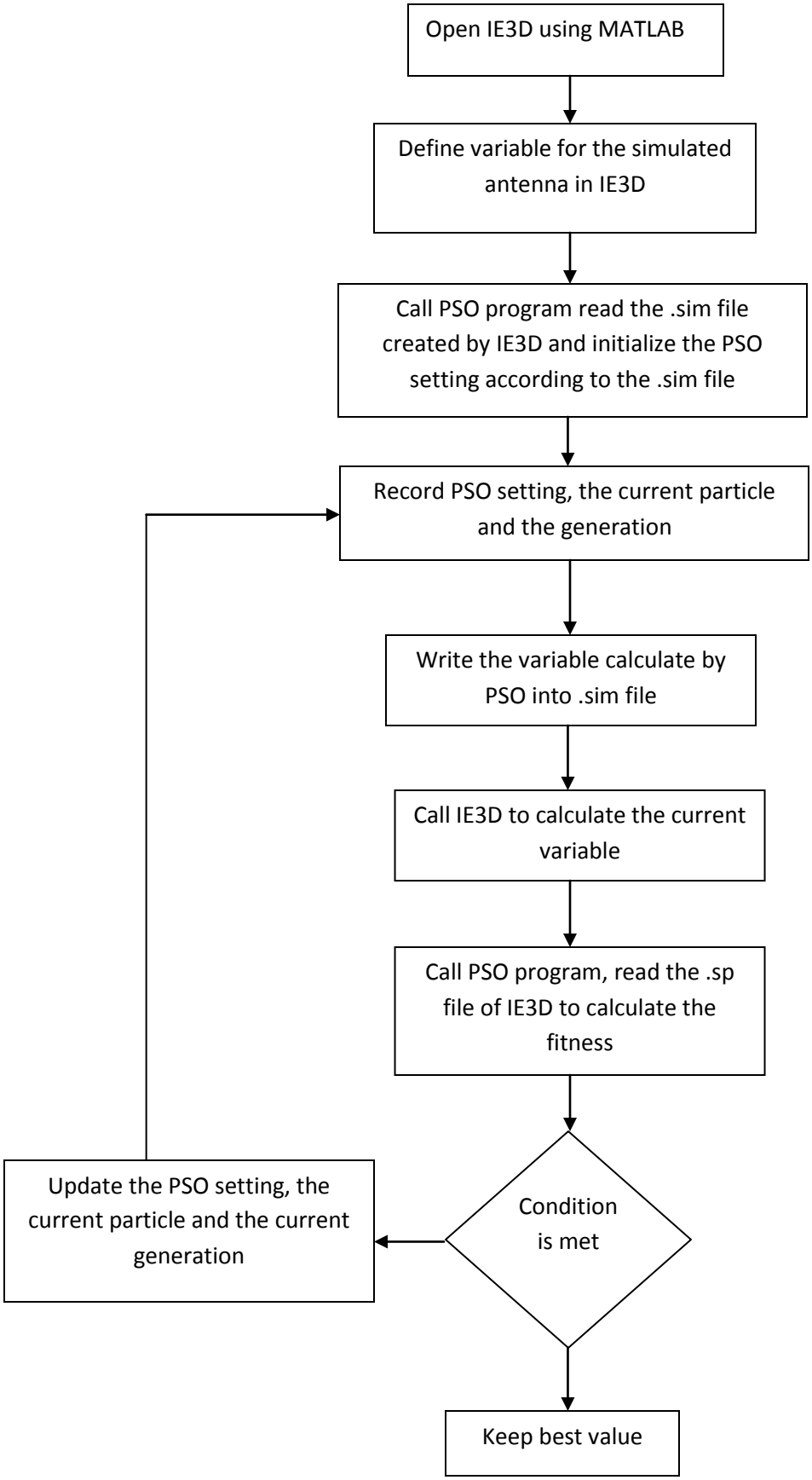

Figure 7.1 Flow chart illustrating the steps of a PSO/IE3D algorithm.

IE3D is a full-wave, method-of-moments-based electromagnetic simulator solving the current distribution on 3D and multilayer structures of general shape. It has been widely used in the design of microwave/mm-wave circuits, patch antennas, wire antennas, and other RF/wireless antennas. Different optimization schemes are available in IE3D, including Powell optimizer, genetic optimizer, adaptive optimizer and random optimizer. The variables for optimization defined by IE3D are controlled by its directions and bounds. However, the variables can only be connected with another by a fixed rate. More complicated relations between variables can not be set in IE3D. Optimization with complicated variations, such as the optimization of the width and slots on a patch simultaneous may cause a overlap problem in IE3D. Design method by combining particle swarm optimization with IE3D is used to obtain the parameters of the Microstrip antenna.

7.2 Optimization of Single Band Antenna using IE3D\PSO

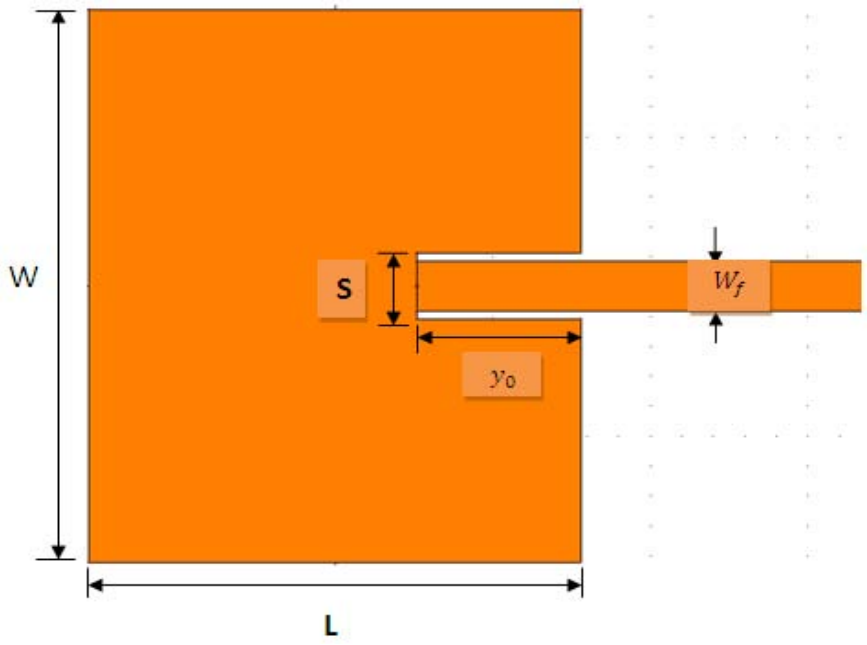

Figure 7.2 Single Band Microstrip Antenna geometry

The geometry of single band Microstrip patch antenna is shown in Figure7.1 .The antenna size is characterized by length (L), width (W) and inset depth (y_0) of the patch and thickness of the substrate material (h). The antenna is fed by inset feeding. The initial design parameters of antenna geometry and its optimized values obtained from the PSO-IE3D methods are listed in Table 7.1.

Bonds	Length	Width	Inset depth
Lower bond	35	40	10
Higher bond	45	50	18

Table 7.1 Optimized bound of single band Microstrip antenna

Particle swarm optimization is a robust stochastic evolutionary computation technique based on the movement and intelligence of swarm, which is very easy to understand and implement. It can be manipulated according to the chapter 6 and following equations in [8]

$$v_{mn} = W * v_{mn} + \varphi_1\, rand\,()\left(p_{mn}^{bp} - x_{mn}\right) + \varphi_2 rand()\left(g_n^{bp} - x_{mn}\right) \quad 7.1$$

And

$$p(\Delta) = S(v_{mn})(1- S(v_{mn})) \quad 7.2$$

where,

v_{mn} =Velocity, p (Δ) =Particle displacement, p_{mn}^{bp}= best position of the partical , g_n^{bp}= global best position of the partical, φ_1& φ_2= are acceleration constant and $rand$ ()= random values. First we set the impedance at 50 Ω for optimized using the following equation 7.1 & 7.2. PSO algorithm uses the fitness evaluation to represent how well a solution satisfies the design parameters. Each parameter used to evaluate the fitness is referred to as a fitness factor. The

fitness factors must together quantify the result. A common means to do this is called the method of weighted aggregation (MWA). The fitness is calculated by

$$F = \sum_{i=1}^{N} W_i f_i$$

Where *N* is the number of fitness factors, f_i is the value of the i_{th} fitness factor, and W_i is a weighting coefficient.

By combining the IE3D-PSO according to the flow chart is shown in figure 7.1.

For single band microstrip patch antenna with resonant frequency is 2.4 GHz. The design parameters are listed in table 7.1. The number of particles is taken as 10 and the number of iteration is 1000 for this combination the fitness function is given by:-

$$Fitness\ function = \min\ (S_{11}^2)$$

The optimized result shown in table 7.2.

Width(mm)	Length(mm)	Inset depth(mm)
46.9	39.4	13.9

Table 7.2 optimized result of Single Band Microstrip Antenna

$\varepsilon_r = 2.4$, h=1.58 mm

7.2.1 Theoretical and PSO Result of Single Band Microstrip Antenna

Single Band Microstrip Antenna theoretical result can be obtained from chapter 4 in table 4.2 where the width, length and inset depth can be calculated by [15]

7.2.1.1 Return loss and Antenna Bandwidth

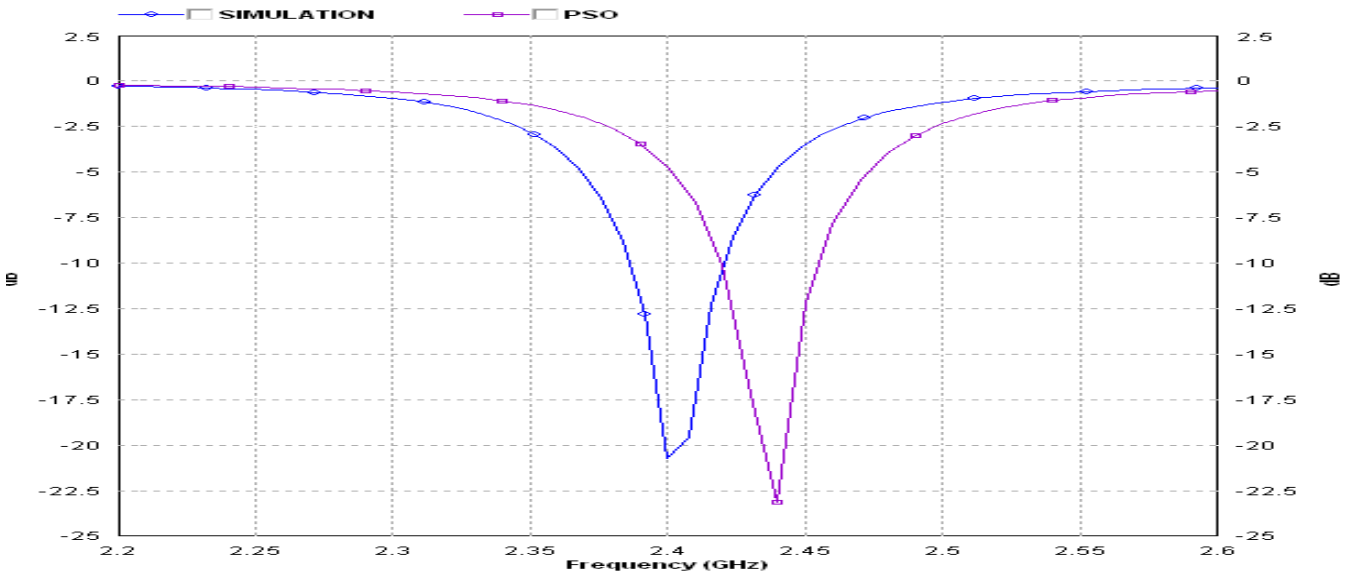

Figure 7.3: Return loss of Theoretical and PSO

7.2.1.2 Radiation Pattern

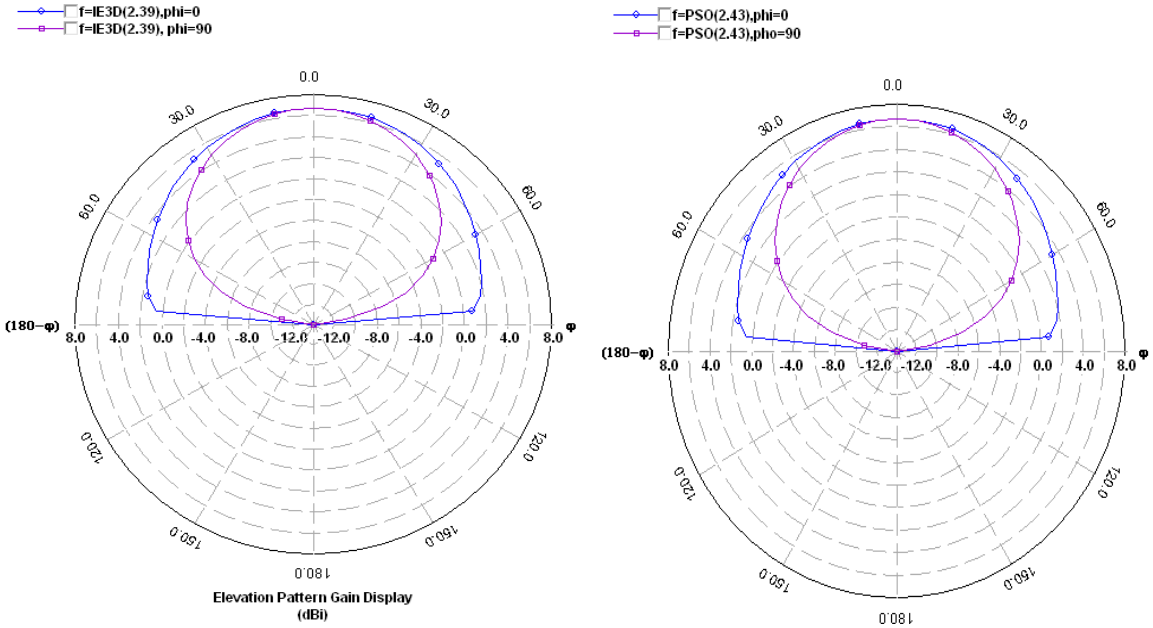

Figure 7.4: Elevation Pattern for Φ=0 and Φ= 90 degrees of Theoretical and PSO

7.2.1.3 VSWR

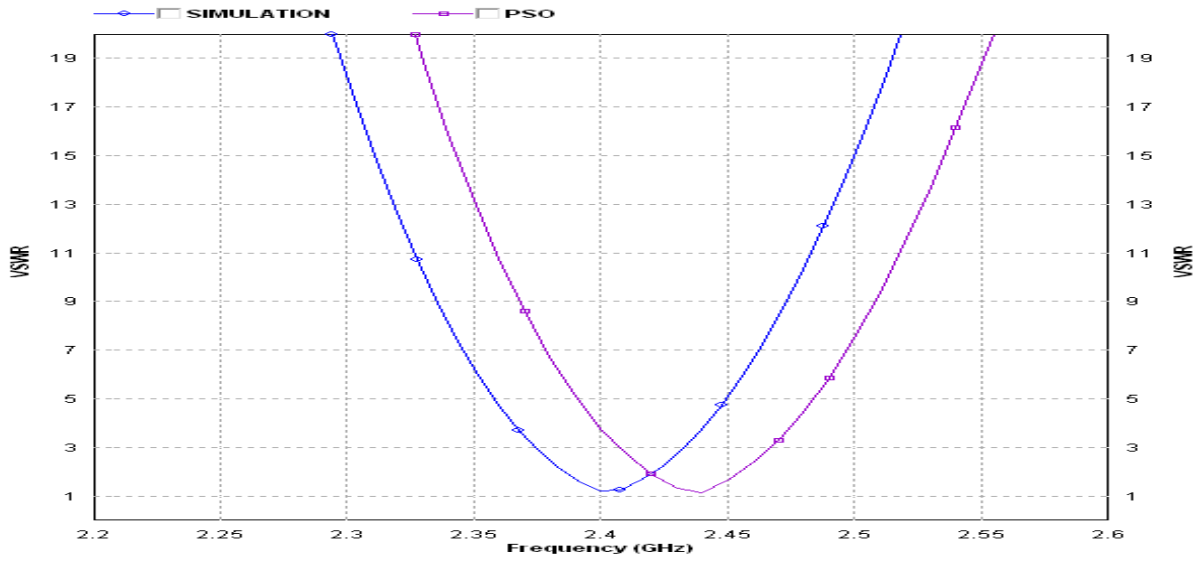

Figure 7.5 VSWR of the theoretical and PSO

7.2.2 Comparison between Theoretical and IE3D\PSO

Parameter	Result	
	IE3D(Simulation)	PSO
Frequency(GHz)	2.4	2.43995
Width	39.6	39.4
Length	46.9	46.9
Inset depth	13.2	13.9

Table 7.3 comparison between Theoretical and IE3D\PSO result

7.3 Optimization of Dual-Band Antenna using IE3D\PSO

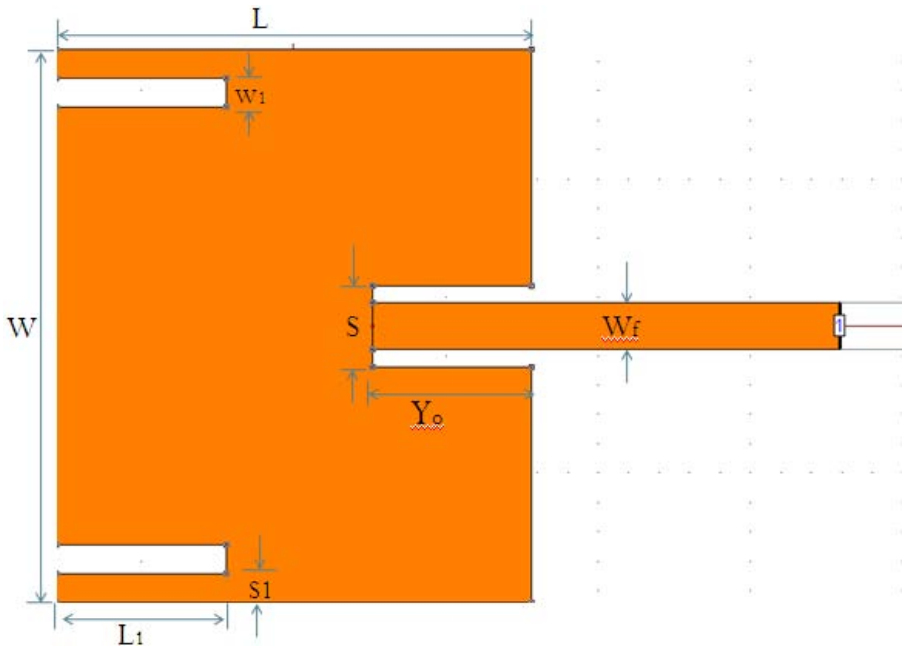

Figure 7.6 Dual-Band Microstrip Antenna geometry

The antenna structure (Fig. 7.6) consists of a rectangular patch with two slots into one of the radiating edges, and is excited using an inset planar feed. The patch design consists of two stages. The first stage involves the creation of an additional $TM_{0\delta}$ resonant mode at a with a resonant frequency above that of the fundamental TM_{01} mode, with the same polarization sense. The second stage is to simultaneously reduce the input impedance of both modes to 50Ω at resonance through the use of an inset feed. This process is taken from chapter 5.

Here we optimize the dual band antenna using the IE3D\PSO. The geometry of Dual Band Microstrip patch antenna is shown in Figure7.6 .The antenna size is characterized by length (L), width (W) and inset depth (y_0) of the patch and thickness of the substrate material (h). The antenna is fed by inset feeding. Two parallel slots near the radiating edges are etched on the patch having a length of L_1 and a width of W_1 to achieve the best-input impedance matching and

minimum return loss. The slots are positioned symmetrically on the patch along its length and width by a separation of l and w respectively. The initial design parameters of antenna geometry and its optimized values obtained from the PSO-IE3D methods are listed in Table 7.3

Bound	Length	Width	Inset depth	Slot length	Slot width
Lower bound	35	40	10	10	10
Upper bound	45	50	18	18	18

Table 7.4 Optimized bound of dual band Microstrip antenna

Applying PSO at Dual Band Microstrip Antenna and calculated the optimized parameter using the equation 7.1 and 7.2.The flow chart is prepared by combining the IE3D-PSO and shown in figure 7.1. Same technique is applied for Dual Band Microstrip patch antenna with resonant frequency is 2.4 GHz.

The design parameters are listed in table 7.3. The number of particle is taken as 10 and the number of iteration is 1000 for this combination the fitness function is given by

$$Fitness\ function = \min\ (S_{11}^2)$$

7.3.1 Theoretical and PSO result of Dual Band Microstrip Antenna

Theoretical results of Dual Band Microstrip Antenna can be obtained from chapter 5 in table 5.1 where the width, length, inset depth, slot length, slot width can be calculated by [1] Optimized result shows in table 7.4. $\varepsilon_r = 2.4$, h=1.58 mm are considered.

Width (mm)	Length (mm)	Inset depth (mm)	Slot length (mm)	Slot width (mm)
46.9000	39.3766	13.9378	14.310	1.4000

Table 7.5 Optimized result of Dual Band Microstrip Antenna

7.3.1.1 Return loss and Antenna Bandwidth

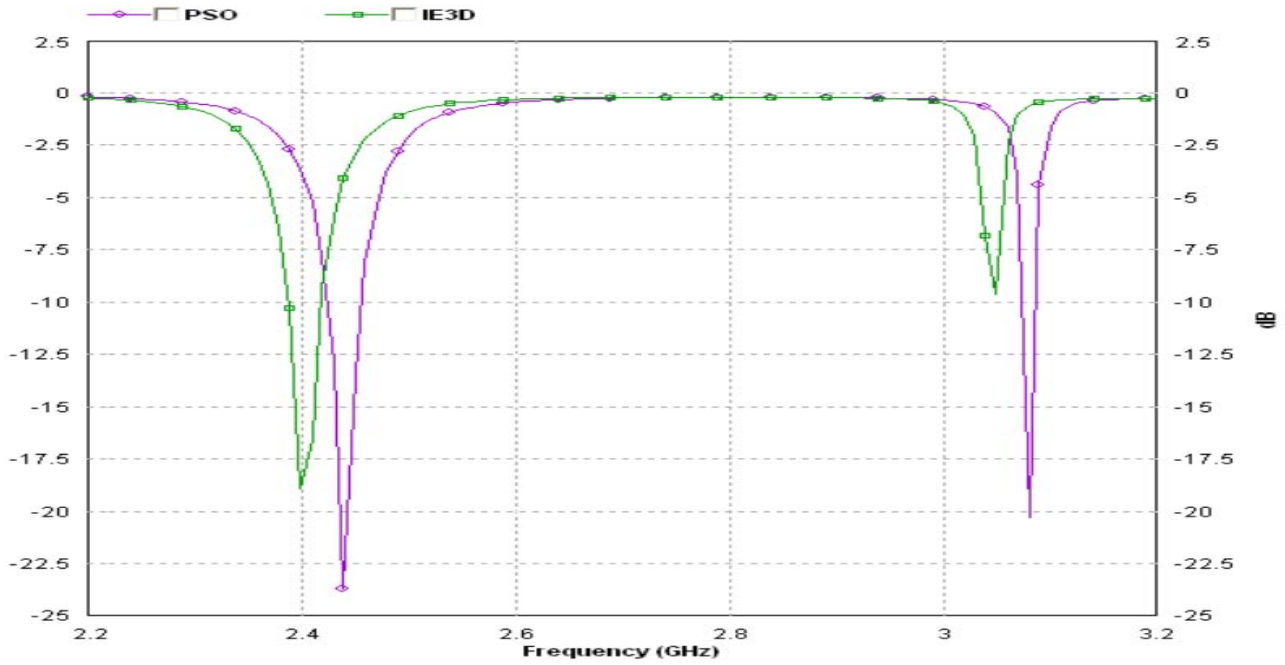

Figure 7.7: Return loss of Theoretical and PSO

7.3.1.2 Radiation Pattern

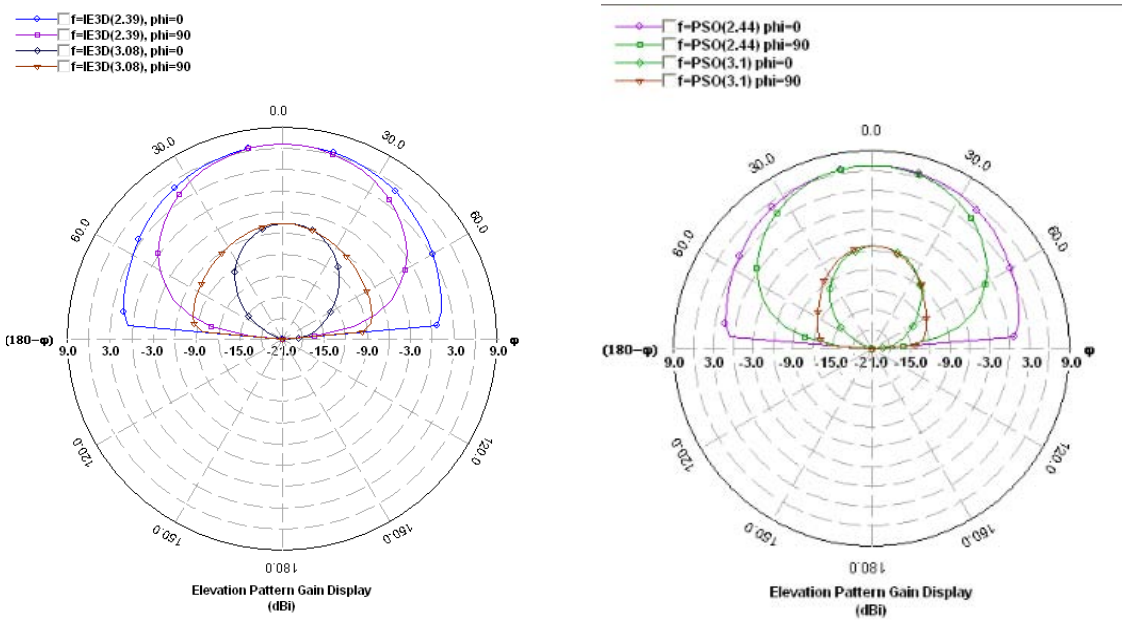

Figure 7.8: Elevation Pattern for Φ=0 and Φ= 90 degrees of Theoretical and PSO

7.3.1.2 VSWR

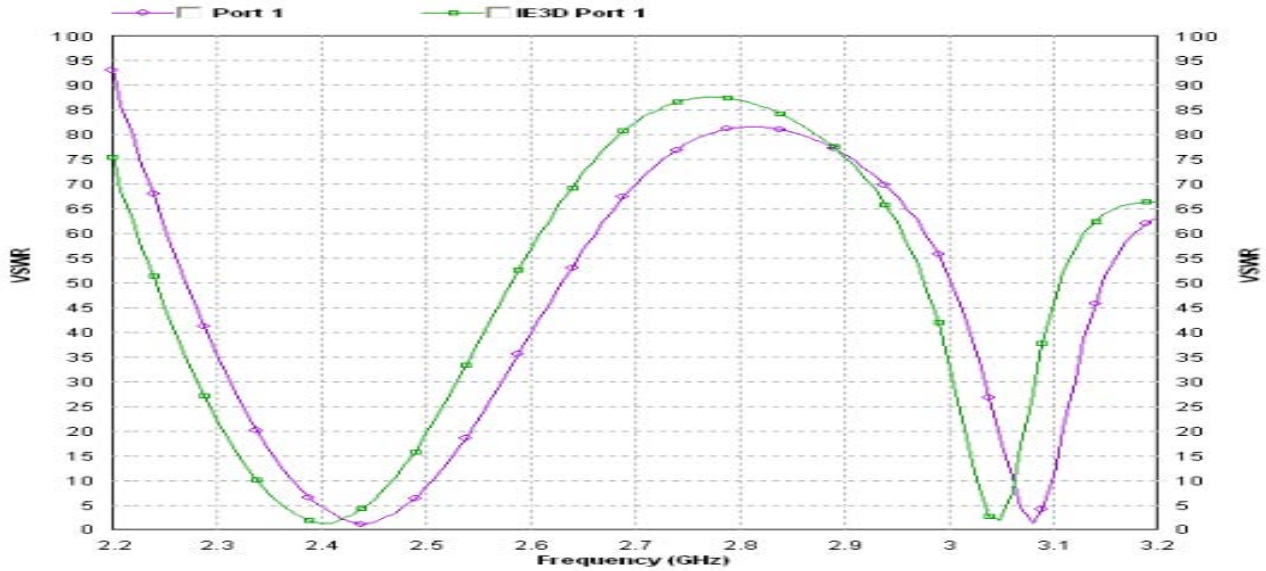

Figure 7.9 VSWR of the theoretical and PSO

7.3.2 Comparison between Theoretical and IE3D\PSO result of Dual Band Microstrip antenna

Parameter	Result	
	IE3D(simulation)	PSO
Frequency(f1)[GHz]	2.39998	2.44003
Frequency (f2)[GHz]	3.10000	3.08003
Width(mm)	39.6000	39.3766
Length(mm)	46.9000	46.9000
Inset depth(mm)	13.2000	13.9378
Slot Length(mm)	14.2000	14.31095
Slot Width(mm)	1.40000	1.40000

Table 7.6 Comparison between Theoretical and IE3D\PSO result of Dual Band Microstrip antenna

CHAPTER 8

CONCLUSION AND FUTURE SCOPE

8.1 Conclusion

Two aspects of Microstrip antennas have been studied in this thesis. The first aspect is the design of typical rectangular Microstrip antenna and the second is the design of dual band Microstrip antenna. A simple and efficient technique of inset method has been introduced for an impedance matching improvement of the antennas. Main concern of the thesis is to study of Dual band patch antenna using different techniques and frequency ratio of the Microstrip antenna. The dual band Microstrip antenna is a more conventional approach for the implementation of a broadband antenna and for satellite communication where the low frequency ratio is used. Initially, single element rectangular Microstrip antenna is designed to operate at frequency 2.4 GHz. And then, the dual band Microstrip antenna is designed to resonate at frequency range 2.4 GHz to 3.08 GHz. The dual band antenna shows that with correct selection of slot dimensions and positions, a dual frequency response can be achieved, while still allowing the use of a planar feed.

The second and very important work is done in this thesis is to implement the single and dual band Microstrip antenna using the interfacing between the IE3D and PSO (MATLAB). The design optimization of a single and dual band rectangular patch antenna has been implemented combining an efficient evolutionary optimization method (PSO) with a standard electromagnetic simulator (IE3D). The accuracy, robustness and ease of implementation of this method validate its potential application in patch antenna design. This method can also be effectively used in the design of various complex microwave and millimeter-wave circuits. The performance of the PSO-IE3D combined antenna design as presented in Figure 7.1 established the fact that IE3D alone is insufficient for precision design of antenna elements for high frequency applications.

8.2 Suggestions for Future Work

Based on gathered observations while completing this thesis; topics were identified which would benefit for further investigation.

- At present facility for fabrication of patch Antenna is not available in our institute; the same work will be performed latter. The simulated, optimized and experimental results will be compared.
- Using the dual frequency Microstrip antenna as a basis, the circular dual frequency Microstrip antenna can be developed. For using the same INSET feeding technique, in terms of wavelength, between the corresponding slots in radiating edge, the "spokes" of the antenna are arranged around the circumference.
- Using the shorting post and changing the slot position in this patch to develop the WLAN concept (2.4 GHz & 5.2 GHz frequency) and also this patch can be used in satellite communication where the low frequency ratio patch is used.
- The first improvement would be to endow the PSO algorithm with a memory for the Fitness of a certain antenna configuration. Since the structures being used in this thesis are relatively small, the penalty for evaluating the same configuration multiple times does not degrade the overall performance significantly. For larger structures, it would however not be acceptable to reevaluate multi-hour runs.

  It would be interesting to include an implementation of the genetic algorithm and thus be able to compare their progress. An elaborate investigation of how the PSO parameters affect this particular antenna optimization is also of interest.

- Using IE3D\PSO method improves the bandwidth of Microstrip antenna. This is the best optimization method to optimized the antenna parameter and overcome the overlapping problem when we optimized the antenna using IE3D optimizer.
- Taking input impedance as part of the PSO algorithm fitness function, the GA can be applied to creates not only a patch antenna that exhibit large size reduction but also reasonability input impedance those are easy to match any feed network.

Appendix

MATLAB Program for Rectangular Patch design

```
%%%%%%%% DESIGN FOR RECTANGULAR PATCH %%%%%%%%
clear all;
close all;
epsilon=input('enter epsilon');
rin0=input('enter the required resistance');
rfreq1=input ('radiation frequency');
rfreq=rfreq1*10^9;
h=input ('enter the thickness of the substrate');
w0=input ('enter the width of the microstrip feed line');
c=2.4*10^10;
w=c/((2*rfreq)*((epsilon+1)/2)^(0.5));
epsilonreff=((epsilon+1)/2)+((epsilon-1)/2)*((1+12*(h/w)))^(-0.5);
deltaL=h*0.412*(epsilonreff+0.3)*((w/h)+0.264)/((epsilonreff-0.258)*(w/h+0.8));
Leff=c/(2*rfreq*(epsilonreff)^(0.5));
L=Leff-2*deltaL;
%.....INSET FEEDING.....
 lamda_o=c/rfreq%wavelength
ko=(2*pi)/lamda_o;
A=(1/(120*(pi^2)));
F1=0;
for theta=[0:1:180]*pi/180
   z=ko*L*sin(theta);
   J = besselj(0,z);
   I =
(((sin((ko*w/2)*cos(theta)))/cos(theta))*((sin((ko*w/2)*cos(theta)))/cos(theta)))*J*((sin(theta))^
3)*(pi/180);
   F1=I+F1;                                    %current (I1=F1)
end
```

```
g12=F1*A;
if (w > lamda_o)
   g1=(1/120)*(w/lamda_o);
end
if (w < lamda_o)
   g1=(1/90)*((w/lamda_o)^2);
end
Rin=(1/(2*(g1+g12)));
if ((w0/h) <= 1)
   Z=(60*(epsilonreff)^(-0.5))*log(((8*h)/w0)+(w0/4*h));
end
if ((w0/h) > 1)
   Z=(120*pi)/((epsilonreff)^(0.5)*((w0/h)+1.393+0.667*log((w0/h)+1.444)));
end
Zc=Z;                                    %calculation for Microstrip line width
Y01=(L/pi).*acos(rin0/Rin)^(0.25);        % calculation for inset depth
```

References

[1]. C.A. Balanis, Antenna Theory, 2nd Ed., John wiley & sons, inc., New York.1982

[2]. Ross Kyprianou, Bobby Yau, and aris, "Investigation into Novel Multi-band Antenna Design", Defence science and technology organization, Australia, 2006

[3]. W. F. Richards, S. E. Davidson, S. A. Long, "Dual-Band Reactively Loaded Microstrip Antenna," *IEEE Transactions on Antennas and Propagation,* AP-33, 5, May 1985, pp. 556-560.

[4]. C.A. Balanis, Advanced Engineering Electromagnetics, John Wiley & sons, New york, 1989.

[5]. E.O. Hammerstad, "Equations for microstip Circuit Design," Pro. Fifth European Microwave Conference, page 268-272, 1975.

[6]. R. Garg,I.J. Bahl, P.Bhartia and A. Ittipiboon, Microstrip antenna Design Hand Book, Artech House, Dedham, MA, 2000.

[7]. Microstrip patch antennas, "*A designer's guide"*, by Rodney B. Waterhouse, 1999.

[8]. S. S. Zhong and Y. T. Lo, "Single Element Rectangular Microstrip Antenna for Dual-Frequency Operation," *Electronics Letters,* 19, *8,* 1983, pp. 298-300.

[9]. S. Maci, G. Biffi Gentili, G. Avitabile, "Single-Layer Dual- Frequency Patch Antenna," *Electronics Letters,* 29, 16, August 1993.

[10]. M. L. Yazidi, M. Himdi and J. P. Daniel, "Aperture Coupled Microstrip Antenna for Dual Frequency Operation," *Electronics Letters,* 29, 17, August 1993.

[11]. S. Maci, G. Biffi Gentili, P. Piazzesi, C. Salvador "A Dual Band Slot-Loaded Patch Antenna," *IEE Proceedings H,* 142, *3,* March 1995, pp. 225-232.

[12]. P. Piazzesi, S. Maci, G. Biffi Gentili, “Dual-Band Dual-Polarized Patch Antennas,” *Znt. MiMiCAE Jour.*, 5, 6, December 1995, pp. 375-384.

[13]. A.G Derneryd, A Theoretical Investigation of the Rectangular Microstrip Antenna Element, IEEE Trans. Antenna Propagation, Vol. 26, No. 4, page 532-535

[14]. Y. Rahmat-Samii and E. Michielssen, *Electromagnetic Optimization by Genetic Algorithms*. John Wiley & Sons, Inc., 1999

[15]. Robinson and Y. Rahmat-Samii, "Particle Swarm Optimization in Electromagnetic". *IEEE Transaction on antennas and propagation*, vol. 52, no. 2, pages 397-407, February 2004.

[16]. James J.R., P.S. Hall and C. Wood. Microstrip Antenna Theory and Design. London, United Kingdom. Peter Peregrinus 1981, pp 87-89.

[17]. J. Kennedy and R. C. Eberhart, "Particle swarm optimization", in *Proc. IEEE Conf. Neural Networks IV*, Piscataway, NJ, 1995.

[18]. D.M. Pozar, microstrip antenna, Proc. IEEE. Vol. 80, No.1, January 1992.

[19]. J. Kennedy and R. C. Eberhart, "A discrete binary version of the particle swarm algorithm", in *Proc. 1997 Conf. Systems, Man, Cybernetics*, Piscataway, NJ, 1995.

[20]. R. Waterhouse, “Small microstrip patch antenna,” Electron. Lett., Vol.31, pp. 604-605,1995.

[21]. Y.Shi and R.C.Eberhart, “Empirical study of particle swarm optimization” Proceedings of the Congress on Evolutionary Computation, pp.1945-1950, 1999.

[22]. X.F Liu et al, “Design of a Low –Profile Modified U Slot Microstrip Antenna Using PSO Based On IE3D”, Proc. Of Microwave and Optical Technology Letters, Vol.49, No.5, pp.1111-1114, May, 2008.

[23]. H. Nakano, K. Vichien “Dual-Frequency Patch Antenna with a Rectangular Notch,” *Electronics Letters*, 25, 16, 1989, pp. 1067-1068.

[24]. D. H. Schaubert, F. G. Ferrar, A. Sindoris, S. T. Hayes, “microstrip Antennas with Frequency Agility and Polarization Diversity,” *IEEE Transactions on Antennas and Propagation*, AP- 29, 1, January 1981, pp. 118-123.

[25]. R. B. Waterhouse, N. V. Shuley, “Dual Frequency Microstrip Rectangular Patches,” *Electronics Letters*, 28, 7, 1992, pp. 606-607.

[26]. S.Maci et al, “Dual-band slot-loaded patch antenna,” IEE Trans. on Microwave Antenna & Propagation, vol. 142, No. 3 , pp. 225-232, June 1995.

[27]. Zeland Software Inc.,”IE3D Electromagnetic Simulation and Optimization Package, Version 9.35”, Zeland Software nc.,Fremont,CA,2003.

[28]. Bhartia P., Millimeter-Wave Microstrip and Printed Circuit Antennas. Norwood, Mass. Artech House 1991.

[29]. W.F. Richards, J.R. Zinecker, R.D. Clark, Taylor and Francis, *Electromagnetics*, Vol.3 No. 3 and 4, p.33.

[30]. J.Y. Szi and K.L. Wong, Slotted rectangular Microstrip antenna for bandwidth enhancement, IEEE Trans Antennas Propagat 48 (2000), 1149–1152.

[31]. J.H. Lu and K.L. Wong, Dual-frequency rectangular Microstrip antenna with embedded spur lines and integrated reactive loading, Microwave Opt Technol Lett 21 (1999), 272–275.

[32]. S. S. Zhong and Y. T. Lo, "Single element rectangular microstrip antenna for dual frequency operation," *Electron. Lett.* vol. 19, no. 8, Pp.298–300, Apr. 1983.

[33]. K.L. Lau, P. Li and K.M. Luk, ''A wideband and dual-frequency shorted patch antenna with compact size'', Antenna and Propagation Society International Symposium, 1, pp. 249–252, 2004.

[34]. S. Bhunia, M. K. Pain, S. Biswas, D. Sarkar, P. P. Sarkar,and B. Gupta, Investigation of Microstrip patch antenna s with different slots and feeding point, Microwave and Optical Technology letters, / Vol. 48, No. 6, August 2008, Pages 2754 – 2758.

[35]. K.P. Yang and K.L. Wong, Dual-band circular-polarized microstrip antenna, IEEE Trans Antennas Propagat 49 (2001), 377–381.

[36]. D.W. Boeringer and D.H. Werner, Particle swarm optimization versus genetic algorithms for phased array synthesis, IEEE Trans Antennas Propag 52 (2004), 771–779.

[37]. D. Gies, "Particle swarm optimization: Applications in electromagnetic design," M.S., Univ. California, Los Angeles, 2004.

[38]. N. Jin and Y. Rahmat-Samii, "Parallel Particle Swarm Optimization and Finite-Difference Time-Domain (PSO/FDTD) Algorithm for Multiband and Wide-Band Patch Antenna Designs," *IEEE Trans. Antennas Propag.,* vol. 53, no. 11, pp. 3459-3468, Nov. 2005.

[39]. Raychowdhury, B. Gupta, and R. Bhattacharjee, "Bandwidth improvement of microstrip antennas through a genetic-algorithm-based design of a feed network," *Micro. Opt. Technol. Lett.* 27(4):273-275 (Nov. 2000).

[40]. O. Ozgun, S. Mutlu, M.I. Aksun, and L. Alatan, "Design of Dual-Frequency Probe-Fed Microstrip Antenna With Genetic Algorithm," *IEEE Trans. Antennas Propagat.*, vol. 51, pp 1947-1954, Aug. 2003.

[41]. J. M. Johnson and Y. Rahmat-Samii, "Genetic algorithms and method of moments (GA/MoM) for the design of integrated antennas," *IEEE Trans. Antennas Propagat.*, vol. 47, pp. 1606-1614, Oct. 1999.

[42]. W. F. Richards, Y. T. Lo, and D. D. Harrison, "An improved theory for microstrip antennas and applications," Rep. RADC-TR-79-11], May 1979, and *IEEE Trans. Antennas Propagat.*, vol. AP-29, no. 1, Jan. 1981.

[43]. N. Fayyaz and S. Safavi-Naeini, Bandwidth enhancement of a rectangular patch antenna by integrated reactive loading, 1998 IEEE AP-S Int Symp Dig, pp. 1100-1103.

[44]. Alikhan, W.F. Richards, and S.A. Lung, Impedance control of Microstrip antennas using reactive loading, IEEE Trans Antennas Propagat 37 (1989), 247–251.

Publication

[1]. **Yogesh Kumar Choukiker, S K Behera,** "Some Results on Dual Band Rectangular Microstrip Antenna ", Proceedings of National conference on Recent Advance in Communication Technology (NCRACT) 2009, page no. 155-156.